Confinement effects within the seismic design of reinforced concrete frames: reliability assessment and comparison

Engineering Structures 313 (2024) 118248

Contents lists available at ScienceDirect

Engineering Structures

journal homepage: www.elsevier.com/locate/engstruct

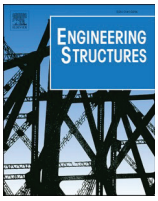

Confinement effects within the seismic design of reinforced concrete frames: reliability assessment and comparison

E. Miceli *, S. Ferrara, P. Castaldo

Department of Structural, Geotechnical and Building Engineering (DISEG), Politecnico di Torino, Turin, Italy

ARTICLE INFO

Keywords:
Design methodology
Reinforced concrete
Confinement models
Ductility
Seismic performance
Seismic reliability

ABSTRACT

The current Italian code "NTC2018" and Eurocode "EC8" provide specific design requirements in terms of flexural overstrength factors for reinforced concrete (RC) buildings in seismic areas. This study proposes to improve the design methodology by including explicitly the confinement effects within the seismic design of a new regular RC frame due to their influence on the capacity design principles (at structural and member level). Specifically, the seismic performance of a RC frame designed according to codes is compared, in reliability terms, with the one of the same frame designed including the concrete confinement effects. Moreover, a comparison between three constitutive models for confined concrete is performed. Selecting L'Aquila (Italy) as reference site, the two design methodologies combined with the three confinement models are numerically implemented. Scaling 30 non-frequent natural ground motions to increasing seismic intensity measures, according to the site seismic hazard, non-linear incremental dynamic analyses (IDAs) have been developed. Assuming the interstory drift indices as engineering demand parameters, the peak responses have been fitted through log-normal distributions to define IDA curves. Subsequently, appropriate limit state thresholds have been adopted to define the seismic fragility curves. Finally, through the convolution integral and Poisson model, the seismic reliability curves have been derived showing the importance of the proposed design methodology. In fact, for the frame under investigation, the seismic performance strongly improves in terms of ductility respecting all the reliability objective levels if the confinement effects are explicitly considered in the seismic design. Furthermore, the different confinement models provide similar results when the proposed seismic design is adopted, implying a reduction of the model uncertainty.

1. Introduction

In the last decades, more attention has been devoted to reliability analysis and design of structures [1] with the aim to improve the structural and seismic assessment of both new and existing reinforced concrete (RC) buildings. To this purpose, the scientific community has progressively developed complex structural models, capable of taking into account the main phenomena that characterize the post-elastic behaviour of RC buildings subjected to seismic actions [2].

Regarding the effects due to the concrete confinement, different researches [3–14] have been conducted over the years showing that factors such as the amount and spacing of confinement steel, the configuration of the longitudinal reinforcement together with the axial load level and position influence the performance of RC elements. In detail, back in the middle 60', Roy and Sozen [5] derived experimentally a bi-linear constitutive law for the confined concrete, underlining the large influence of the spacing of the stirrups on the ductility and the minor influence of the reinforcement percentage as well as of the disposition of the longitudinal reinforcement. Later in the 80', Sheikh and Uzumeri [9] were the first who considered the influence of stirrups' spacing and distribution as well as the disposal of the longitudinal bars not only in the ductility but also in the peak resistance of the confined concrete. Successively, Mander et al. [11] elaborated a stress-strain law including the effects of strain rate and cyclic loading, defining the concept of an effectively constrained area. Furthermore, Saatciouglu and Razvi [13] provided the definition of an equivalent lateral pressure dependent on the arrangement of the stirrups. Most recently, Montoya et al. [15] proposed a new set of constitutive models to include 3D effects, strength enhancement, concrete dilatation, post-peak softening or increased strain hardening in the stress-strain curve of the confined concrete.

In this context, the research project [16] investigated the

* Corresponding author.
E-mail address: elena.miceli@polito.it (E. Miceli).

https://doi.org/10.1016/j.engstruct.2024.118248
Received 6 November 2023; Received in revised form 27 February 2024; Accepted 17 May 2024

performance of the confining steel requirements through a comparison between different code relationships and literature models on the results of multiple reverse-cyclic column tests with respect to a performance target. In [17], experimental tests have been conducted on RC columns confined with two layers of stirrups having different geometrical characteristics regarding both the cross-section type and stirrups spacing. The tests were analysed in terms of load-displacement relationship, strength and stiffness degradation, ductility and dissipated energy achieving no obvious results. Moreover, the confinement effects have also been included within deteriorating hysteretic rules to investigate the cyclic dissipation of the seismic energy by beam-column joints of RC frames, especially in existing structures, taking into account the cyclic deterioration of both stiffness and strength as well as pinching [18].

In addition to deterministic and experimental analyses, another important aspect is represented by the different uncertainties characterising the confined concrete in RC structures, especially, in seismic areas. Probabilistic analyses have been more and more combined with non-linear simulations for RC structural elements to account for the different sources of uncertainty, both epistemic and aleatory, in modelling, in seismic inputs and in the definition of structural parameters [19–23]. A statistical analysis is performed in [24], for the estimation of the probable flexural strength of ductile RC columns considering the uncertainties in material, sectional properties and analytical modelling for different confinement levels. Probabilistic non-linear models for concrete beam-column joints with transverse reinforcement have been proposed in [25]. The high level of uncertainty associated with earthquake characteristics, mechanical uncertainties for both concrete and reinforcing steel were investigated in [26]. An in-depth seismic fragility assessment of RC frame structures has been carried out in [27] considering the uncertainties in both structural parameters and seismic excitations through response surface models, calibrated on the results from several non-linear incremental dynamic analyses (IDAs) with different sets of ground-motions. In [28], the seismic response of a six story RC frame was analyzed for three earthquake records and two confined models provided by [29,30] in order to obtain an insight into the response of the structure, depending on the confined model of concrete.

Nowadays, seismic design of new RC structures, according to codes rules [29–32], imply significant sources of overstrength based on the capacity design principles [33]. The strength at the global or structural level is guaranteed by means of a ductile failure mechanism by the strong column - weak beam principle. At the same time, ductility should be verified at the member level by the hierarchy between shear and flexural behaviour. In fact, flexural strengths are increased by means of appropriate coefficients γ_{Rd}, the so-called overstrength factors, which account for the possibility that the demand is higher than expected one due to material overstrength. However, the calibration of γ_{Rd} derives primarily from the variability of actual yield strength and from the strain hardening of reinforcement [33], rather than from the concrete strength contribution. Other works have instead shown that not considering the variability of concrete strength in the evaluation of γ_{Rd} can be non-conservative [34]. Furthermore, many researchers have shown that the current design code requirements may not guarantee the strong column - weak beam capacity design principle in RC structures [35–37], due to the influence of plastic rotation of beams and columns, joint locations and frame heights. When columns are subjected to high axial load levels, the contribution of concrete overstrength can be more significant [24,38]. However, seismic code [30] imposes the following limitations on the design axial load ratio for columns: 0.55 and 0.65 for high and medium ductility class, respectively.

In this study, the seismic reliability is assessed for a RC frame designed in a high ductility class and for the same frame designed including explicitly the confinement effects in the design due to their influence on the capacity design principles (at structural and member level). In addition, three different confinement models [11,13,31–32] are investigated. The seismic reliability assessment of the two frames is compared within the three confinement models. In detail, non-linear incremental dynamic analyses (IDAs) [39] with 30 non-frequent seismic inputs are developed in SAP2000 [40]. Selecting the interstory drift indices (IDIs) as the Engineering Demand Parameters (EDPs), the seismic fragility is defined considering appropriate limit state thresholds. Finally, for the frame under investigation, the seismic reliability curves have shown the effectiveness of the proposed design methodology in improving the seismic performance in terms of ductility with respect to the fulfilment of all the code limit states and in reducing the model uncertainty regarding the confinement effects.

2. Standard seismic design and proposed seismic design methodology

This section deals with the design of the RC frame following two approaches: i) one considering the conventional design approach of the Italian code NTC2018 [31,32], in line with the European ones [29,30] (i.e., standard seismic design) and, ii) another one including the confinement effects on the concrete compressive response at structural and member level (i.e., proposed seismic design).

2.1. Standard seismic design

An ordinary RC building (i.e., class II [31,32]) located in the highly seismic area of L'Aquila (Italy) and composed of three stories is considered. The materials are C25/30 for concrete and B450C for reinforcing steel regarding beams, columns and joints, according to [31,32] for new structures. The partial safety factors γ_c= 1.5 and γ_s = 1.15 are used for concrete and reinforcing steel, respectively. The considered RC moment resisting (MR) frame is shown in Fig. 1 with the geometrical details: spans of 5 m, interstory height of 3 m and transverse influence width of 5 m. The frame is located on a ground "type B" with a topographic category "T1" and PGA values of 1.02 g for operational limit state (LS) (i.e., a return period of 50years) and 2.56 g for life safety LS (i.e., a return period of 475years) [30–32]. The behaviour factor q_0 equal to 5.85 is adopted considering high ductility class with α_u/α_1 ratio equal to 1.3 for multi-storey multi-bay frames [30–32].

As for the new regular 2D RC MR frame under investigation (Fig. 1) and considering the Italian code NTC2018 [31,32], in line with European codes [29,30], elastic static and modal analyses were carried out in order to design the structural elements together with the longitudinal and transversal steel reinforcement rebars according to the different load combinations related to the four LSs: Fully Operational (FO) LS, Operational (O) LS, Life Safety (LS) LS and Near Collapse (NC) LS in the hypothesis of high ductility class [30]. The following overstrength factors [30] are adopted: 1.2 for shear verifications of beams, 1.3 for shear and compressive-bending verifications of columns and 1.2 for shear verifications of beam-column nodes. Note that all the structural elements (i.e., beams, columns and joints) have been verified as well as the inelastic verifications required for the NCLS have also been performed, according to the codes [30–32].

Regarding the actions, the following values are assumed: 18 kN/m for the slab being 4 cm thick and composed of one-way joists having a height of 16 cm, 21 kN/m for the surcharge dead load and 10 kN/m or 2.5 kN/m for the live load on the floors or on the roof, respectively.

In this way, without considering the confinement effects within the standard seismic design, the non-linear behaviour of concrete has been considered unconfined according to the codes [30–32]. Consequently, the rectangular cross-section of all the beams is 40x50cm^2 with Φ8/70 vertical stirrups in the dissipative zones for a length of 750 mm from the beam-column joint and has the following longitudinal reinforcement bars: 3Φ24 above and 2Φ22 below. In the non-dissipative zones, the stirrups spacing is 150 mm.

For the columns, the rectangular cross-section is 50x60cm^2 with 14Φ20 as longitudinal reinforcement bars, located doubly symmetrical with respect to the orthogonal barycentric axes, and Φ8/120 stirrups in

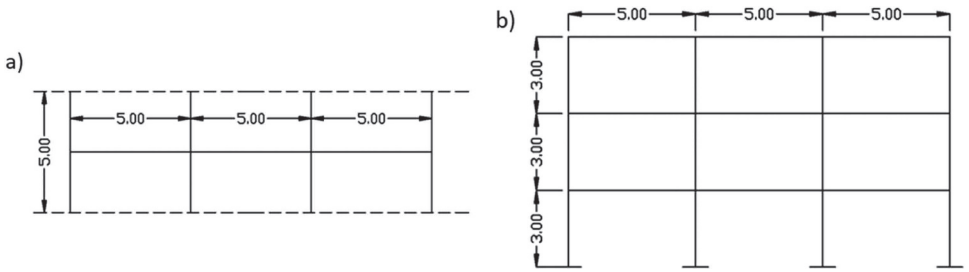

Fig. 1. 2D RC MR frame: a) plane view of the transverse influence width and b) front view. Measurements in meters.

the dissipative areas for a length of 600 mm from the beam-column joint. In the non-dissipative zones, the stirrups spacing is 200 mm. The legs have the same diameter and spacing of the stirrups as a function of the dissipative or non-dissipative zones.

The highest dimensions of both the cross-sections are within the frame plane (Fig. 2). All the code provisions regarding the construction details have been checked. The longitudinal reinforcement layout is constant along the entire length of each beam and column.

The clear concrete cover is equal to 40 mm for all the structural elements. Fig. 2 shows the longitudinal reinforcements of the frame, the stirrups and legs together with the beam and column cross-sections.

2.2. Proposed seismic design methodology considering confinement models

This subsection describes the proposed design methodology finalised to consider explicitly the confinement effects at structural and member level in the seismic design process of new RC buildings. Both the overstrength and behaviour factors are the same adopted in the standard seismic design. The frame under investigation has been re-designed according to the codes by considering explicitly the concrete confinement effects. Specifically, in order to consider the non-linearity in the behaviour of both the unconfined and confined concrete material, the following three constitutive laws have been assumed:

- model by Saatcioglu & Razvi [13], based on Hognestad model [3], denoted as “model 1”;
- model by Mander et al. [11], defined as “model 2”;
- NTC2018/parabola-rectangle model [31,32], in line with [29], assumed as “model 3”.

The three models define the constitutive laws for both the unconfined concrete (i.e., clear concrete cover) and confined concrete as a function of the stirrups and legs in any structural member. These three confinement models can lead to differences in the design since they can influence the ultimate resistance verifications as well as the fulfilment of the capacity design principles at structural and member level [30–32]. After an iterative procedure, it follows that, for the frame under investigation, there is a modification in all the beams to respect the shear verifications because of the overstrength in flexural resistance: the

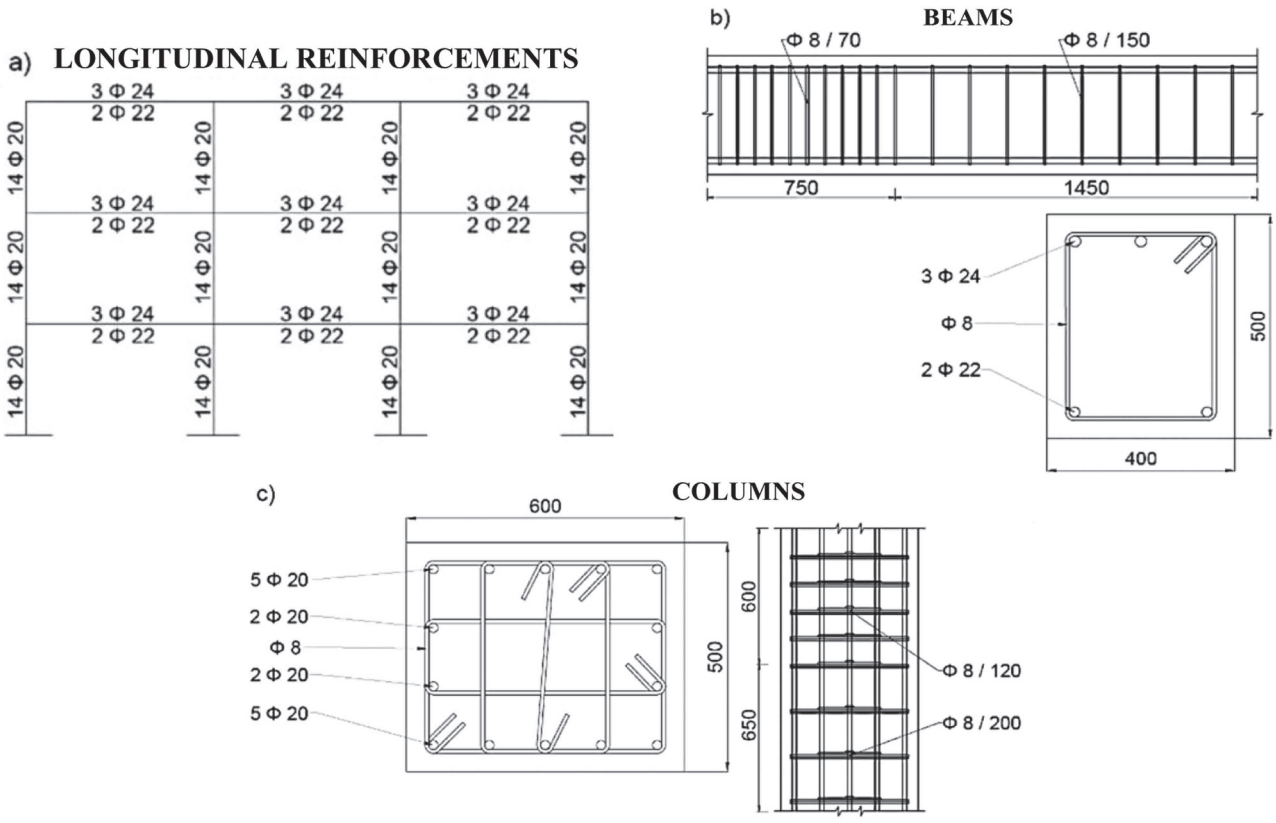

Fig. 2. Standard seismic design: a) layout of the longitudinal reinforcement rebars of the RC MR frame, b) stirrups with the cross-section of the beams and c) stirrups and legs with the cross-section of the columns. Measurements in millimetres.

spacing of the vertical stirrups decreases from 70 mm to 50 mm in the dissipative zones 750 mm long from the beam-column joint at each extremity. Regarding the other details of beams, columns and joints, there are not modifications. Fig. 3 shows the transversal reinforcement modification in the beams: this design solution is effective for all the three confined models.

The two seismic design approaches are different because the proposed methodology needs an iterative procedure since it takes into account the increased design value of the peak stress in compression, combined with the increased ultimate strain, of the confined concrete in the ultimate verifications. In fact, the design values of the ultimate resistance bending moments of the cross-sections of any beam are higher and can influence, consequently, the ultimate shear verifications according to the capacity design principles at member level [30–32]. In addition, this last effect can also affect the design values of the ultimate resistance bending moments of the cross-sections of the connected columns and the related ultimate shear verifications according to the capacity design principles at structural level [30–32]. Accordingly, these modifications can influence the shear demand acting in the column above the joint and, consequently, the ultimate shear verifications of the joints.

By means of two flow-charts, Fig. 4 presents the comparison between the standard seismic design, followed in the previous subsection, and the proposed seismic design methodology including explicitly the concrete confinement effects.

For the frame under investigation, within both the seismic design approaches, it should be underlined that, considering a ψ_2 of 0.3 (for residential category of use), and unitary partial safety factors for all the loads in seismic combination, the internal columns are subjected to a design axial load ratio υ_d slightly lower than 0.2, in line with [30]. In addition, by performing the joint checks within the seismic combinations [30–32], the following minimum and maximum design values of column-to-beam overstrength ratios (i.e., $\Sigma M_{Rd,b}/\Sigma M_{Rd,c}$) are, respectively, obtained: 0.147 and 0.392 for the standard seismic design, whereas 0.153 and 0.403 for the proposed approach (similar for the three confinement models). These values are quite identical between the standard seismic design and proposed seismic design. It follows that, for the frame considered, the proposed seismic design implies modifications in the application of the capacity design principle at member level due to the overstrength in flexural resistance leading to a higher number of stirrups in the beams. This leads mainly to a more ductile response of the beams and of the frame under investigation.

3. Incremental dynamic analyses (IDAs): Structural model, seismic records and numerical results

3.1. Numerical structural model

With the aim to assess the seismic reliability of the RC MR frame by comparing the two seismic design methodologies and three confinement models, six different non-linear numerical models have been defined in SAP2000 [40] taking into account both the mechanical and geometrical non-linearities. Note that the mean values for the mechanical properties have been considered accounting for the different responses of the confined concrete in the structural elements. In fact, each numerical model corresponds to a specific design methodology with a particular model for the confined concrete. For the models related to the standard seismic design, the confinement effects are implemented to perform the reliability assessment, whereas for the models related to the proposed seismic design, the confinement effects derive from the design phase.

As for concrete material and considering the mean values of the mechanical properties together with the confinement effects, Fig. 5 shows the constitutive laws for concrete in compression and in tension through stress-strain curves with respect to the cross-sections in the structural elements (i.e., beams and columns) as function of the two design methodologies.

Regarding the compression behaviour, Fig. 5 represents and compares the three confinement models [11,13,31–32] (i.e., model 1, model 2 and model 3) for the two design methodologies. Furthermore, each subplot of Fig. 5 depicts the constitutive laws used for the clear concrete cover (i.e., unconfined concrete - UC) of any structural element and those for the confined concrete (CC) referred, respectively, to beams and columns, designed according to the standard seismic design and proposed seismic design methodology, separately.

In addition to the intrinsic differences between the three confined laws, it can be noted that the standard design approach, based on the UC constitutive law, leads to confined responses shown in Fig. 5a),c),e), whereas the proposed design approach is based on both the UC and CC laws and leads to the results of Fig. 5b),d),f). It is noteworthy that the proposed methodology leads to an increase of the peak stress in compression and of the ultimate strain in the beam cross-sections with respect to the standard seismic design. The confinement "*k*" factors are also reported in Fig. 5 indicating the ratio between the mean values of the peak strengths related to the CC and UC laws. Note that the *k* factors for the two design approaches are the same regarding the columns since there are not differences in the arrangement of the shear reinforcement.

As for the concrete tensile behaviour, an elastic model up to a peak stress [11,31–32] with a post-peak linear tension softening is considered, where the tension stiffening effect is included by means of a linear post-peak branch up to the zero strength defined according to [19]. Fig. 5 also shows the tensile laws considering the mean values of the mechanical properties.

Regarding the reinforcing steel in the longitudinal and transversal rebars, the constitutive law is a bi-linear model with a hardening law both in tension and in compression (Fig. 6), in agreement with [31,32]. In detail, the yield strength is equal to 489 MPa, while the ultimate-to-yield strength ratio is equal to 1.15 [31,32]. The ultimate strain is equal to 7.5 % [31,32].

The non-linear behaviour of the structural elements is modelled through hinges with distributed plasticity (i.e., fiber plastic hinges) arranged at the ends of each beam and column. The length of each plastic hinge has been defined according to [41]. Moreover, regarding hysterical models for concrete and reinforcing steel materials, the concrete hysteresis is considered through the Takeda model [42]; instead, the steel hysteresis is considered through a kinematic hardening behaviour [40].

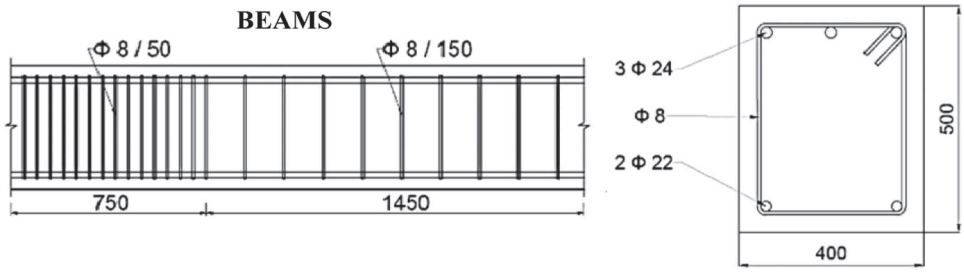

Fig. 3. Proposed seismic design: stirrups with the cross-section of the beams. Measurements in millimetres.

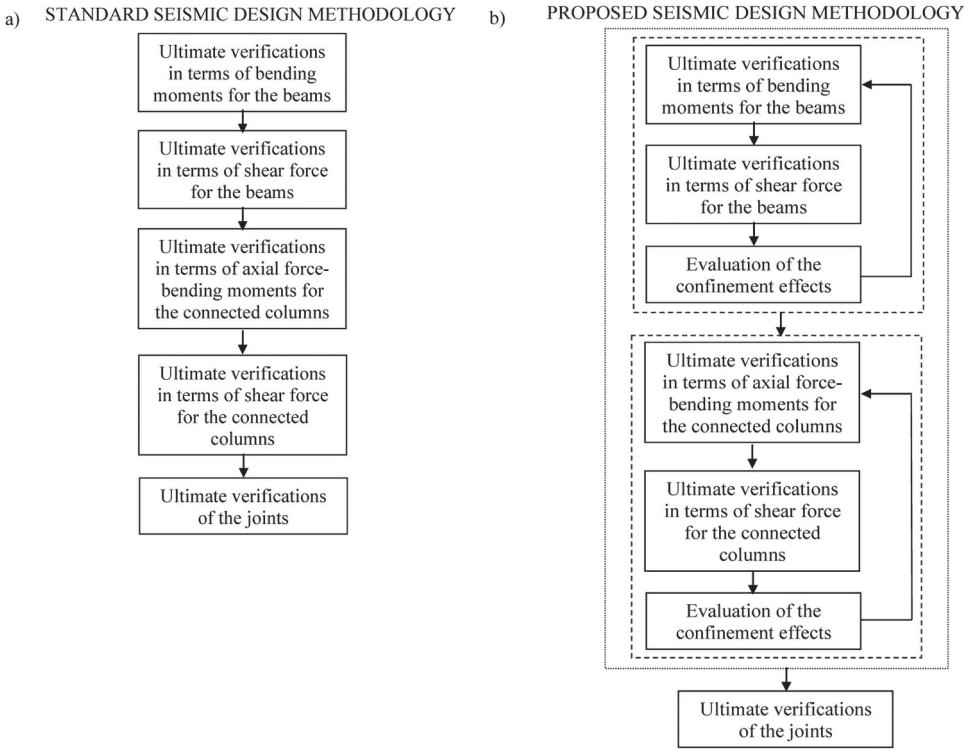

Fig. 4. Flow-charts of the two methodologies for seismic design of new RC buildings: a) standard seismic design and b) proposed seismic design with the confinement effects.

Fig. 7 depicts the numerical model of the 2D RC MR frame together with the discretization in fibers of the beam and column cross-sections, in SAP2000 [40]. The number of fibers along the two directions has been determined after an iterative procedure of numerical accuracy (Fig. 7-b)).

To validate the design assumptions, non-linear static analyses (i.e., pushover analyses) of the six different non-linear numerical models have been developed leading to the following "α_u/α_1" ratios, respectively, for the standard and proposed seismic design: 1.15 and 1.16 (model 1), 1.16 and 1.19 (model 2), 1.13 and 1.16 (model 3), which are in line with the values assumed in the design [30–32]. The results also show a higher ductility capacity of the frames related to the proposed seismic design. In addition, the pushover analyses confirm the level of axial force in the beams due to the horizontal actions with an average value equal to 150 kN in the non-linear phase of the response. It follows that the parameter α_X, corresponding to the confinement effectiveness in the formulation by [43], is around 0.22 and 0.24 for the beams considering, respectively, the standard and proposed methodology and 0.32 for the columns. These α_X values lead to modified confined concrete laws [43] quite in line with the ones described previously (Fig. 5). Note that the model 1 (Fig. 5) leads to the highest increase in the stress peak for confined concrete at strain values higher with respect to the other two models. In addition, the model 1 presents the highest slope in the post-peak branch.

An inherent damping factor equal to 5 % has been considered by means of Rayleigh model to perform the non-linear dynamic analyses able to capture both the uncertainty in the seismic input and effects due to higher modes useful for the reliability assessment. In this way, the possible advantages of the proposed seismic design, which can play an important role under extreme events, can be appreciated.

3.2. Seismic records

This subsection describes the ground motions. In detail, 30 non-frequent natural ground motions have been selected to account for the uncertainties in the seismic input (i.e., record-to-record and event-to-event variability: 30 various records belonging to 20 different earthquake events) [44–47] to perform the IDAs. The characteristics of the records are listed in Table 1. Other details may be found in [21].

3.3. Numerical simulations and results

With the aim to carry out IDAs, an intensity measure (IM) needs to be introduced into the reliability analysis to consider the uncertainties of the seismic input intensity, since the uncertainties on the characteristics of the records are taken into account through the set of natural ground motions, as described in the previous subsection. In this work, the chosen IM is the spectral elastic pseudo-acceleration at the fundamental period: $S_a(T)$ [48,49]. Particularly, the fundamental period T represents the period of the first vibration mode, i.e., $T_1 = 0.31$ s, and is assumed essentially equal for all the six different numerical models although very low differences in the elastic branches between the confined concrete laws according to the three models within the two design methodologies (Fig. 5). Ten increasing values of the $S_a(T)$, common to all the six non-linear numerical models, have been selected in the range [0;1.0 g] with a step of 0.1 g in order to scale the records according to the seismic hazard of the reference site (i.e., L'Aquila, Italy). The maximum value for the IM has been chosen equal to 1.0 g since $S_a(T)$ is 0.865 g in the hypothesis of a reference lifetime equal to 50 years in relation to the NCLS [31,32].

Other uncertainties are not considered since the aim of the study is to compare the two seismic design methodologies together with the three confinement models. Therefore, this seismic reliability assessment represents a seismic demand hazard assessment since it contains only one source of aleatory uncertainty related to the seismic records. It is worthy to underline that if, on the one hand, neglecting other aleatory uncertainties tends to underestimate the failure probabilities, on the other hand, employing all non-frequent records leads to overestimate the failure probabilities, especially, for low IM levels [50]. In addition, the underestimation should not be very relevant since the RC MR frame,

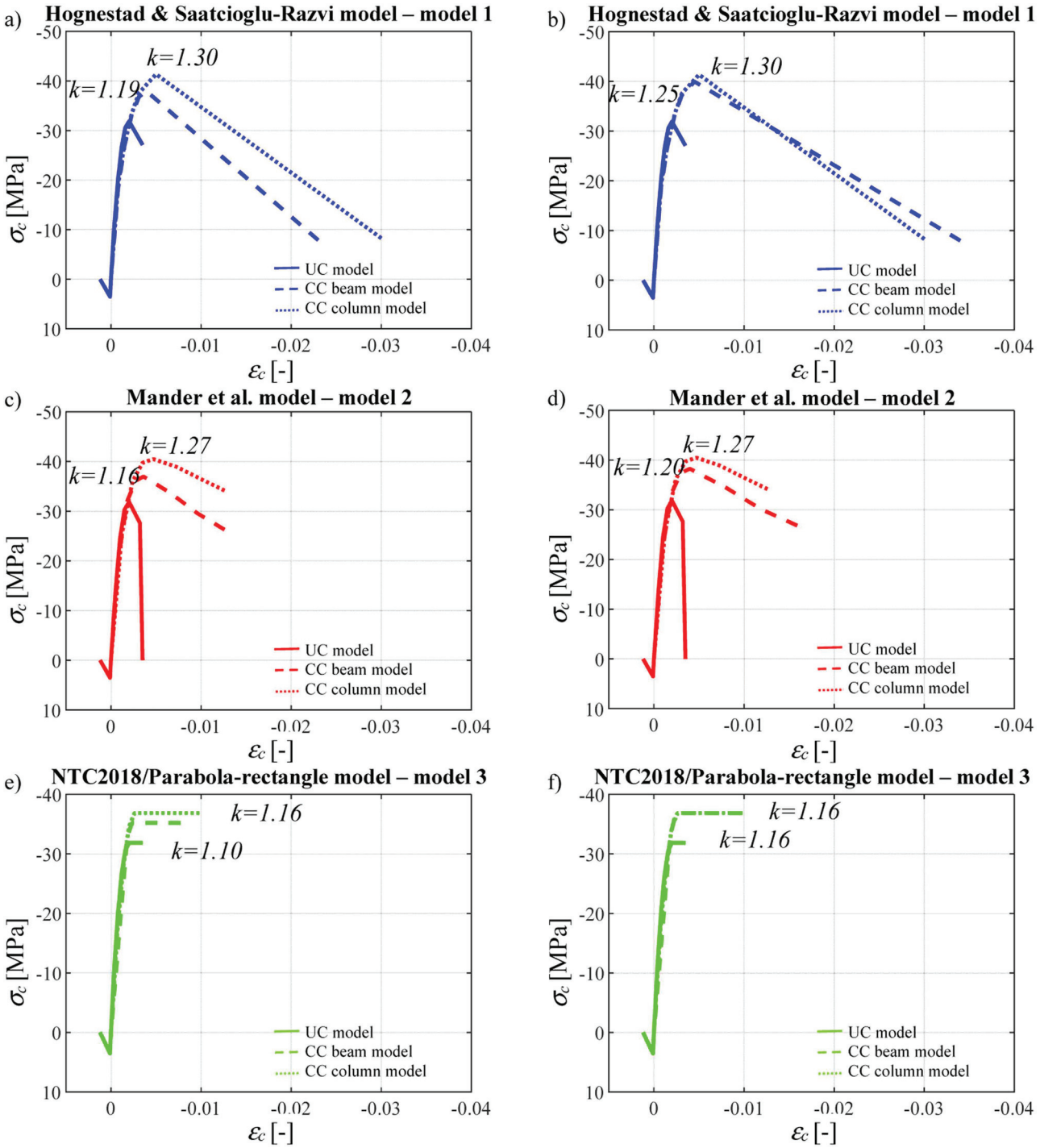

Fig. 5. Comparison between the UC, CC beam and CC column models considering the standard seismic design (left) vs the proposed seismic design (right): a)-b) "model 1", c)-d) "model 2" and e)-f) "model 3".

designed in a high ductility class, should present a non-linear ductile response and, so, the coefficient of variation deriving from material uncertainties should not be so high [51–53]. Regarding the modelling uncertainties, the comparison between the three models representing the confined concrete behavior falls within the epistemic uncertainties assessment in seismic field [19].

Within the abovementioned hypotheses, one IDA, corresponding to one of the six numerical structural models, consists of 300 non-linear simulations, using the 30 seismic records scaled to the 10 different IM (i.e., $S_a(T)$) values. The IDAs allow estimating the Engineering Demand Parameters (EDPs). The adopted EDPs are ductility-related parameters: the peak interstory drift index (IDI) at each one of the three levels of the structure (i.e., IDI_1, IDI_2, IDI_3) and the peak IDI in the building (i.e., between the different levels: IDI_{max}). This last EDP has been assumed as an enveloped response parameter and is mainly influenced by both IDI_1 and IDI_2. It is important to specify that if a collapse occurred at any floor, the IDIs do not exist and neither IDI_{max}. Note that the collapse cases correspond to occurrence of numerical instabilities due to flexural mechanisms with material failure or to the non-fulfilment of the shear verifications for cyclic loads [30–32,54–56] of the structural components (i.e., beams and/or columns and/or joints). These last verifications have been performed considering the results from the non-linear IDAs.

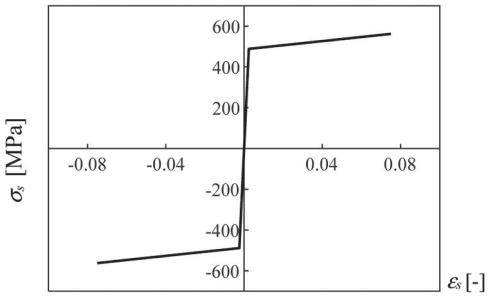

Fig. 6. Constitutive model of the reinforcement steel.

These failures have not been considered in the computation of the statistics in the IDA curves but have been accounted for in the fragility assessment [50,57–58], as discussed in the next section. In Table 2, the number of collapses for each numerical model is shown at each IM level. The highest number of collapses occurred in the standard seismic design due to the shear verifications for cyclic loads, especially, in the beams. By comparing the confinement models, the model 1 and model 3 lead to higher number of collapses due to the higher values in the peak stage for the model 1 and the lower ultimate deformation for the model 3.

The response parameters from the IDAs are assumed to follow a lognormal distribution [19,50,59–63]. This distribution allows to estimate the response in terms of different percentile levels [19,50,59–63]. The lognormal distribution is fitted by estimating the sample lognormal mean $mean_{\ln}(EDP)$ and sample lognormal standard deviation $\sigma_{\ln}(EDP)$ through the maximum likelihood estimation method in MATLAB [64],

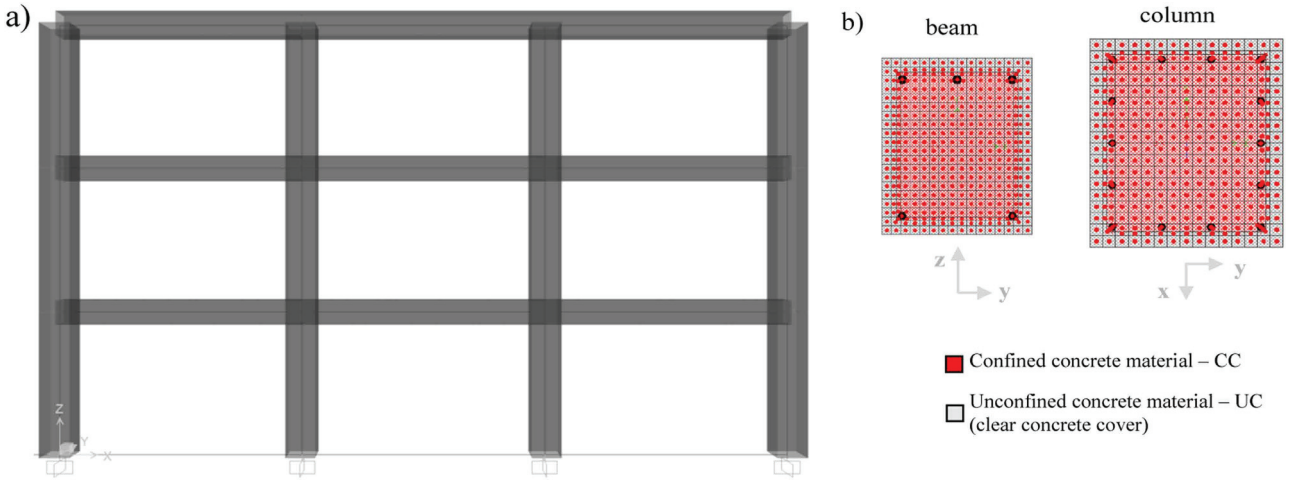

Fig. 7. a) 2D numerical model, b) the beam and column cross-sections discretized in fibers.

Table 1
Characteristics of the 30 selected ground motions.

#	Year	Earthquake name	Recording station name	Vs30 [m/s]	Fault type	M [−]	Rs [km]	PGA [g]
1	1994	Northridge	Beverly Hills-Mulhol	356	Thrust	6.7	13.3	0.52
2	1994	Northridge	Canyon Country-WLC	309	Thrust	6.7	26.5	0.48
3	1994	Northridge	LA-Hollywood Stor	316	Thrust	6.7	22.9	0.36
4	1999	Duzce, Turkey	Bolu	326	Strike-slip	7.1	41.3	0.82
5	1999	Hector Mine	Hector	685	Strike-slip	7.1	26.5	0.34
6	1979	Imperial Valley	Delta	275	Strike-slip	6.5	33.7	0.35
7	1979	Imperial Valley	El Centro Array #11	196	Strike-slip	6.5	29.4	0.38
8	1995	Kobe, Japan	Nishi-Akashi	609	Strike-slip	6.9	8.7	0.51
9	1995	Kobe, Japan	Shin-Osaka	256	Strike-slip	6.9	46.0	0.24
10	1999	Kocaeli, Turkey	Duzce	276	Strike-slip	7.5	98.2	0.36
11	1999	Kocaeli, Turkey	Arcelik	523	Strike-slip	7.5	53.7	0.22
12	1992	Landers	Yermo Fire Station	354	Strike-slip	7.3	86.0	0.24
13	1992	Landers	Coolwater	271	Strike-slip	7.3	82.1	0.42
14	1989	Loma Prieta	Capitola	289	Strike-slip	6.9	9.8	0.53
15	1989	Loma Prieta	Gilroy Array #3	350	Strike-slip	6.9	31.4	0.56
16	1990	Manjil, Iran	Abbar	724	Strike-slip	7.4	40.4	0.51
17	1987	Superstition Hills	El Centro Imp. Co.	192	Strike-slip	6.5	35.8	0.36
18	1987	Superstition Hills	Poe Road (temp)	208	Strike-slip	6.5	11.2	0.45
19	1987	Superstition Hills	Westmorland Fire Stat.	194	Strike-slip	6.5	15.1	0.21
20	1992	Cape Mendocino	Rio Dell Overpass	312	Thrust	7.0	22.7	0.55
21	1999	Chi-Chi, Taiwan	CHY101	259	Thrust	7.6	32.0	0.44
22	1999	Chi-Chi, Taiwan	TCU045	705	Thrust	7.6	77.5	0.51
23	1971	San Fernando	LA-Hollywood Stor	316	Thrust	6.6	39.5	0.21
24	1976	Friuli, Italy	Tolmezzo	425	Thrust	6.5	20.2	0.35
25	1980	Irpinia	Bisaccia	496		6.9	21.3	0.94
26	1979	Montenegro	ST64	1083	Thrust	6.9	21.0	0.18
27	1997	Umbria Marche	ST238	n/a	Normal	6.0	21.5	0.19
28	2000	South Iceland	ST2487	n/a	Strike-slip	6.5	13.0	0.16
29	2000	South Iceland (a.s.)	ST2557	n/a	Strike-slip	6.4	15.0	0.13
30	2003	Bingol	ST539	806	Strike-slip	6.3	14.0	0.30

Table 2
Collapse numbers for the two seismic design methodologies and three confinement models.

		IM [g]									
		0.1	0.2	0.3	0.4	0.5	0.6	0.7	0.8	0.9	1.0
Standard seismic design	**Model 1**	-	-	-	-	-	-	-	4	7	8
	Model 2	-	-	-	-	-	-	-	1	3	7
	Model 3	-	-	-	-	-	-	-	3	5	8
Proposed seismic design	**Model 1**	-	-	-	-	-	-	-	-	-	1
	Model 2	-	-	-	-	-	-	-	-	-	1
	Model 3	-	-	-	-	-	-	-	-	-	2

excluding the collapse cases (Table 2).

Fig. 8 - Fig. 10 represent the IDA curves corresponding, respectively, to the four IDIs for the three confinement models within the two seismic design approaches (i.e., the standard seismic design and proposed seismic design). Each plot represents the EDP values in terms of the corresponding peak IDI for the 30 natural earthquakes scaled to the 10 IM values, excluding collapse cases [30–32,54–56]. It is evident that the IDA curves are different between the four IDIs. For almost all the IM levels, the EDP at the first floor IDI_1 (Fig. 8-a),b), Fig. 9-a),b), Fig. 10-a), b)) presents the highest values in terms of dispersion, whereas the EDP at the second floor IDI_2 (Fig. 8-c),d), Fig. 9-c),d), Fig. 10-c),d)) presents almost always the highest mean values. Regarding the EDP IDI_3, it always presents the lowest values in terms of both mean and dispersion. With reference to the EDP IDI_{max}, it is an enveloped parameter and is influenced mainly by the EDP IDI_2 and, for few IM levels, the statistical values also depend on the EDP IDI_1.

Note that the occurrence of collapse cases (Table 2) strongly influences the statistics of the probabilistic distributions, especially, at high $S_a(T)$.

As for the standard seismic design, the curves, respectively, of the 16th, 50th and 84th percentiles present a lower slope for increasing $S_a(T)$ values higher than $S_a(T) = 0.7$ g. So, the collapse cases affect the IDA curves of the three floors (Fig. 8-a),c),e),g) - Fig. 10-a),c),e),g)).

As for the proposed seismic design methodology, it is possible to observe a reduction in the slope of the IDA curves for IM values higher than $S_a(T) = 0.9$ g (Fig. 8-b),d),f,)h), Fig. 9-b),d),f,)h), Fig. 10-b),d),f,)h)). This reduction of the slope in the IDA curves only for very high $S_a(T)$ values implies a decrease of the number of collapse cases, and, consequentially, this means that the design including the confinement effects is able to improve the seismic response ensuring the fulfilment of the shear verifications for cyclic loads [30–32,54–56] for beams, columns and joints.

By comparing the standard seismic design and proposed seismic design, the IDA curves related to the standard approach appear lower due to the higher number of collapse cases, since they have been excluded in the computation of the statistics of the EDPs. The relevant reduction of failures within the proposed methodology depends on the higher mechanical properties characterising the structural elements. In fact, the peak and ultimate properties of the elements designed with the confinement modifications are higher (Fig. 3) with the consequential respect of the seismic cyclic load verifications for beams, columns and joints. At the same time, the structural elements can dissipate more energy with a different redistribution of the internal actions leading to a reduction of the collapses.

Within the same design methodology, by comparing the results of the three confinement models, it is observed a similar trend of the IDA curves with some differences in both the numerical response and collapse cases. Specifically, within the standard seismic design, differently from the models 1 and 3, the model 2 leads to collapses for higher IM levels (i.e., higher than 0.8 g) with the consequence that the models 1 and 3 present a higher number of collapses (Table 2). Within the proposed seismic design methodology, the model 3 presents the highest results with a slight increase of collapses at IM= 1.0 g (Table 2). This means that the non-linear responses of the structural models have been different under the variability of the seismic excitations up to collapse demonstrating a non-negligible influence the confinement models on the IDA results.

4. Seismic fragility assessment

According to the Performance Based Earthquake Engineering (PBEE) approach [44–46,65–69], the seismic reliability assessment is the comparison between the "Performance Objective" (PO) curve and "Structural Performance" curves within the "Performance Space" or "Design Space" [70,71].

The PO curve is referred to specific performance levels or LSs. In agreement with [55,65,70,72], the four code LSs (i.e., FOLS, OLS, LSLS and NCLS) [30–32,54–55,65,72], can be identified by means of specific LS thresholds in terms of IDI_{LS} values, as listed in Table 3. In order to assess the seismic reliability of the RC MR frame with a high ductility class and compare the two design methodologies, a value of 2.5 % as LS threshold for the NCLS has been selected.

With the aim to define the structural performance curves, it is necessary to evaluate the seismic fragility, defined as the probability P_f exceeding the LS thresholds at each IM level. The fragility evaluation has been carried out taking into account both the collapse and not-collapse cases using the total probability theorem, according to [50,57–58,63], as follows:

$$P_f(IM = im) = \left(1 - F_{EDP|IM=im}(LS_{EDP})\right).\frac{N_{not-collapses}}{N} + 1.\left(\frac{N_{collapses}}{N}\right) \quad (1)$$

where $F_{EDP|IM=im}(LS_{EDP})$ represents the probability of not exceedance of the LS threshold (i.e., IDI_{LS}) for the specific EDP (i.e., IDI) at a given IM level, N is the overall number of numerical analyses at each IM level, $N_{not\text{-}collapses}$ is the number of simulations successfully finalised and not characterised by any collapse (Table 2), and $N_{collapses}$ is the complementary of $N_{not\text{-}collapses}$ with respect to N and represents the cases of numerical instabilities for flexural mechanisms with material failure or failures of the cyclic load verifications, previously described (Table 2). The probabilities exceeding the different LSs (i.e., IDI_{LS}) at each IM level have been fitted through lognormal complementary cumulative distribution functions (CCDFs). The R-square values are always higher than around 0.80 confirming the effectiveness of the fitting process.

Fig. 11-Fig. 14 represent the seismic fragility curves related to both the standard seismic design and proposed seismic design methodology for the different EDPs and concrete confinement models (i.e., models 1, 2 and 3).

From Fig. 11-Fig. 14, it is noteworthy to observe important differences between the two design methodologies in terms of exceeding probabilities. Moreover, the seismic fragility curves related to the four LSs highlight some differences between the three different confinement models, especially, for high LS thresholds with a non-linear structural response (i.e., LS3 and LS4). In addition, the seismic fragility curves are also different by comparing the EDPs corresponding to the different IDIs.

Focusing on the LS1 (Fig. 11), the probabilities P_f exceeding the LS threshold for the EDP IDI_1 are very similar to the highest values of the EDP IDI_2 increasing for IM level higher than $S_a(T) = 0.5$ g. The P_f values are the lowest for the EDP IDI_3, in accordance with the IDA curves. The

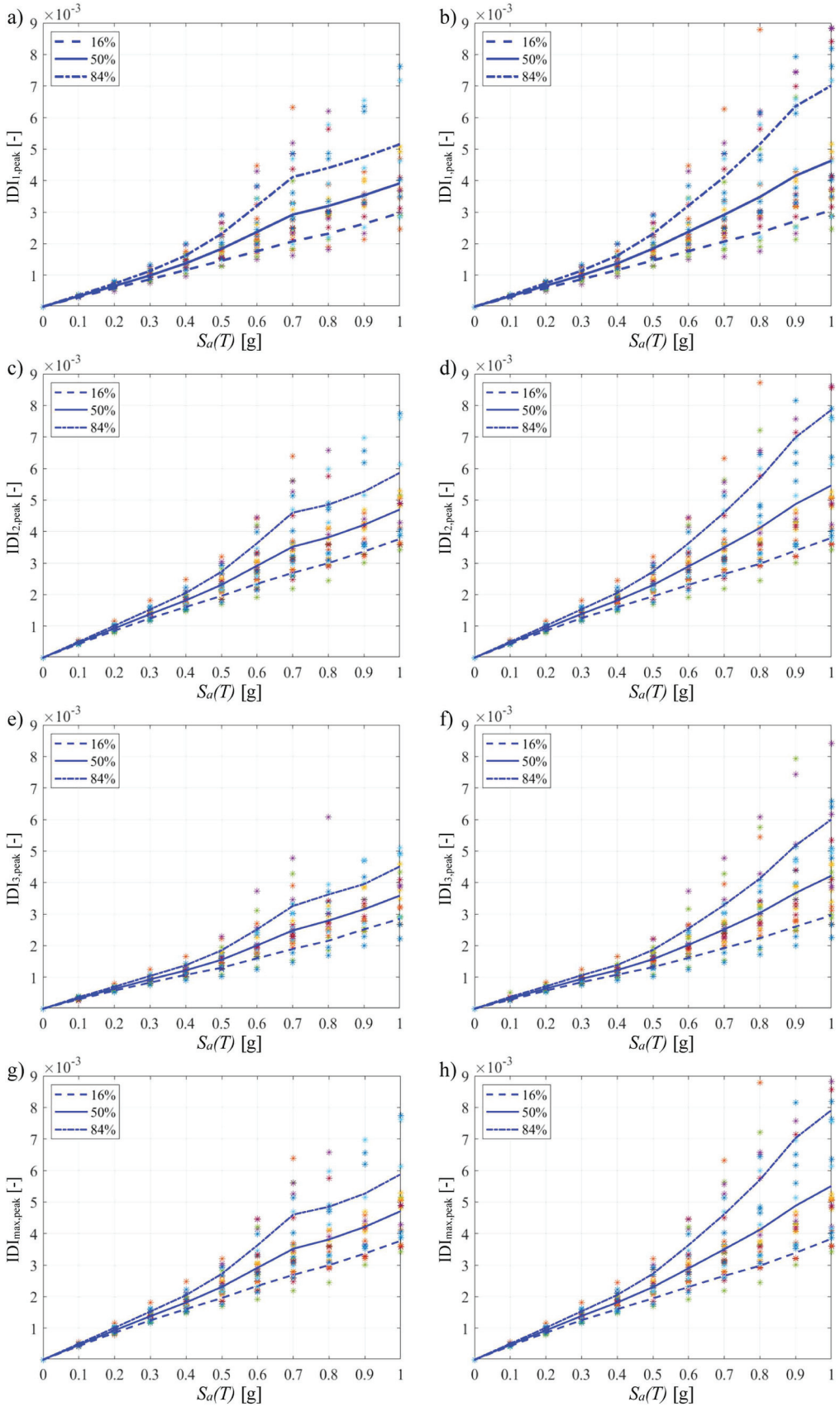

Fig. 8. IDI of the a)-b) 1st story, c)-d) 2nd story, e)-f) 3rd story and g)-h) maximum, referred to the "model 1" considering the standard seismic design (left) and the proposed seismic design (right).

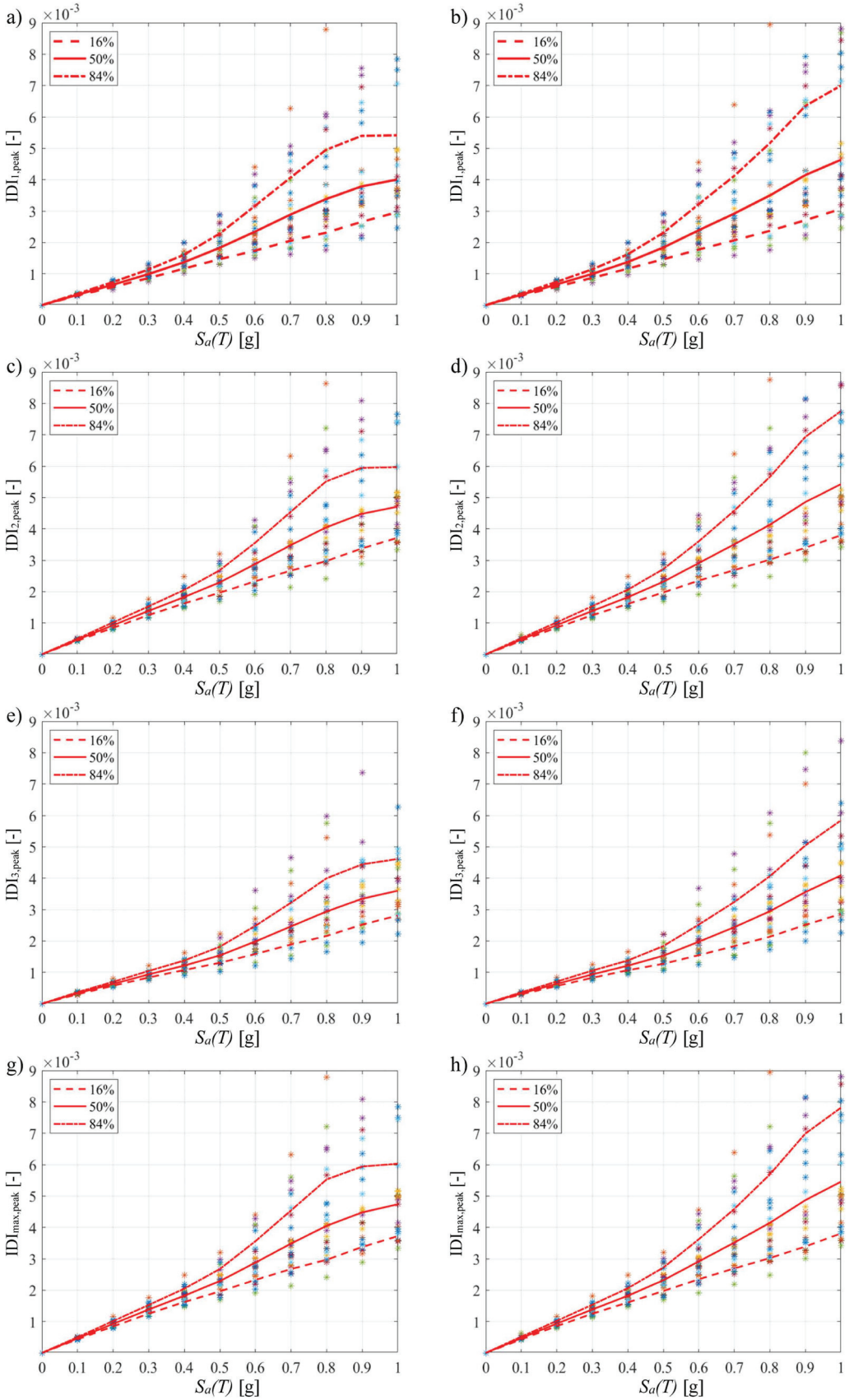

Fig. 9. IDI of the a)-b) 1st story, c)-d) 2nd story, e)-f) 3rd story and g)-h) maximum, referred to the "model 2" considering the standard seismic design (left) and the proposed seismic design (right).

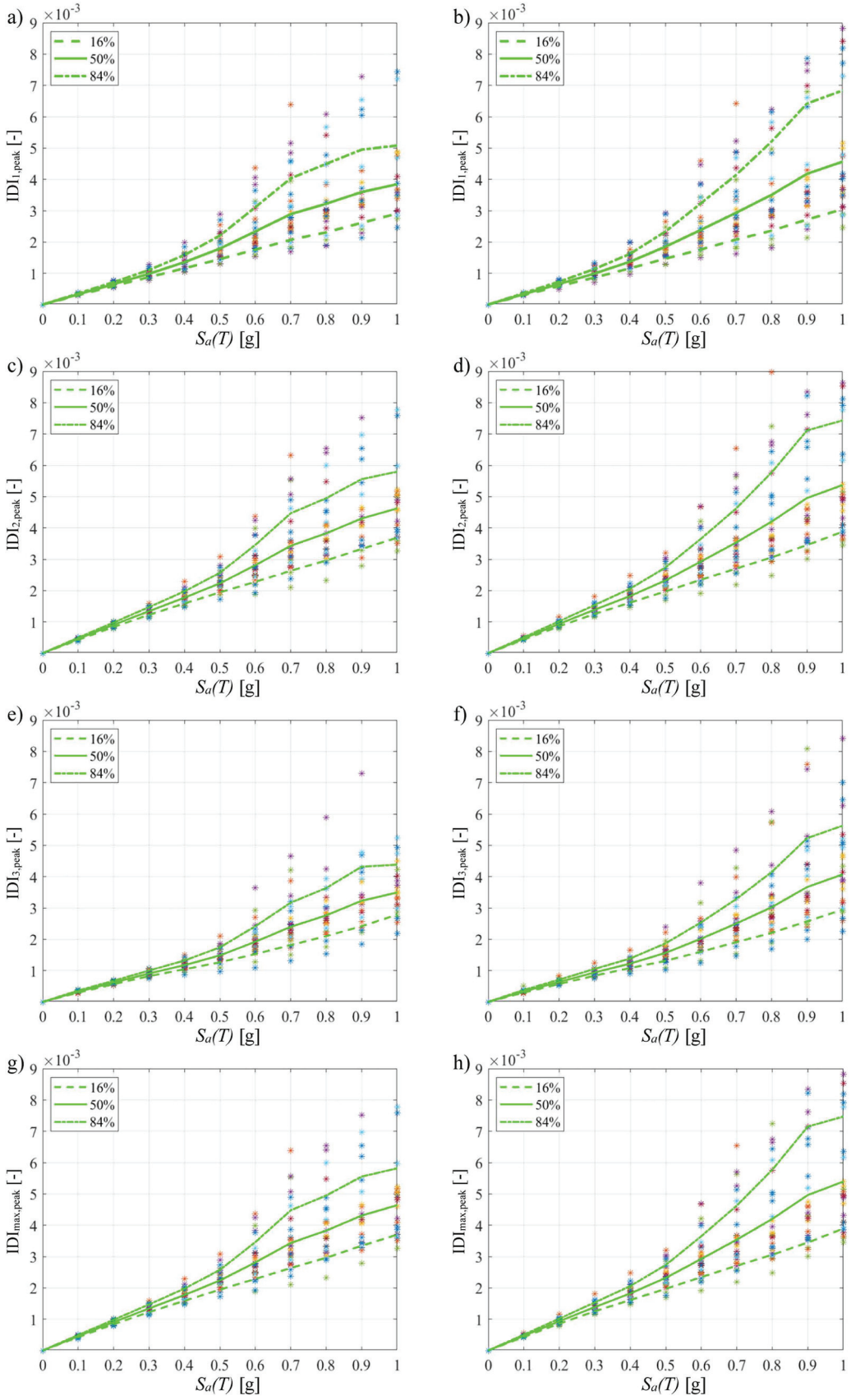

Fig. 10. IDI of the a)-b) 1st story, c)-d) 2nd story, e)-f) 3rd story and g)-h) maximum, referred to the "model 3" considering the standard seismic design (left) and the proposed seismic design (right).

Table 3
Limit States in terms of IDI_{LS} [55,65,70,72].

Performance Level	Limit State	IDI_{LS} [%]
Fully Operational	LS1	0.30
Operational	LS2	0.60
Life Safety	LS3	1.50
Near Collapse	LS4	2.50

fragility curves corresponding to the EDP IDI_{max} are very similar to the EDP IDI_2. These considerations are true both for the standard seismic design and proposed seismic design as well as for the three confinement models. The exceeding probabilities are quite similar between the two design methodologies.

As for the LS2 (Fig. 12), the exceeding probabilities P_f increase for $S_a(T)$ values higher than 0.6 g and are the lowest for the EDP IDI_3, as noted for the LS1. The highest values between the three floors correspond to the EDP IDI_2 that mainly influences IDI_{max}. Also for this LS2, the exceeding probabilities are quite similar between the two design methodologies. Considering the standard seismic design approach for any EDP, the seismic fragility curves related to the model 1 (i.e., Saatcioglu & Razvi model) depict values higher than both the model 2 (i.e., Mander et al. model) and model 3 (i.e., NCT2018/Parabola-rectangle model). In contrast, considering the proposed seismic design approach for any EDP, the seismic fragility curves are very similar between the three confinement models with slightly higher values related to the model 3 (i.e., NCT2018/Parabola-rectangle model), in agreement with the IDA results.

In addition to the fitting model uncertainty, the abovementioned low differences between the two design methodologies in the LS1 and LS2 mainly depend on the characteristics of the records combined with the very low differences of the elastic branches between the confined concrete laws according to the three models. Moreover, within the standard approach the transition towards the non-linear branch starts for lower stress levels.

Regarding the LS3 and LS4 (Fig. 13-Fig. 14), since the LS thresholds increase, the failure probabilities P_f strongly decrease. The differences between the standard seismic design and proposed seismic design are more and more evident. Indeed, the failure probabilities P_f are much lower within the proposed approach for the three concrete confinement models, particularly, the order of magnitude is lower. In fact, as illustrated in Fig. 8-Fig. 10 and Table 2, the collapse cases for the proposed design approach are lower for the higher resistances and ductility capacities of the structural elements. Fig. 13-Fig. 14 show that the seismic fragility curves increase for IM levels higher than $S_a(T) = 0.7$ g for the three confinement models. In detail, the lowest results correspond to the EDP IDI_3, whereas the highest values are referred to the EDP IDI_1 combined with the model 1 (i.e., Saatcioglu & Razvi model) within the standard seismic design. In these cases, the EDP IDI_{max} is strongly influenced by the EDP IDI_1. As also observed for the LS2, this result derives from the higher dispersion of the IDA curves combined with the higher number of collapse cases. Differently, as for the proposed seismic design including explicitly the confinement effects, the model 3 (i.e., NCT2018/Parabola-rectangle model) leads to the highest values according to the IDA curves.

5. Seismic hazard curve

Considering the site of L'Aquila in Italy, Fig. 15 shows the seismic hazard curve expressing the mean annual rate (MAF) of exceedance λ_c of the various IM levels considered in this study. This curve, plotted in semi-logarithmic scale, has been specifically derived for the site, where the structure is located, by following the procedure described in the Italian seismic code [31,32] and according to the data from the National Institute of Geophysics and Volcanology (INGV) website [73]. Table 4 contains the values of λ_c as a function of the pseudo-accelerations corresponding to the fundamental elastic period of the structure $S_a(T)$.

6. Seismic reliability curves

After the seismic fragility assessment, it is possible to evaluate the seismic reliability of the RC MR frame in the performance space through a comparison of the SP curves with the PO curve [70,71]. According to the several guideline documents, code provisions and literature studies [50,55,63,65–70,72], relationships between the four structural PO levels, expressed in terms of the EDP for each LS, and the corresponding reliability indices, β, or probabilities exceeding the LS thresholds during the lifetime (i.e., 50 years) of the structure [74], have been established. Specifically, these correlations are presented in Table 5 in agreement with both International [30,55,65,72] and Italian seismic code [31,32] provisions. In this way, the PO curve is defined in terms of the four LSs considered (i.e., LS1, LS2, LS3 and LS4) with the associated probabilities exceeding the LS thresholds in 50 years, as reported in Table 5.

The SP curves, herein representative of seismic demand hazard curves since include only the aleatory uncertainties related to the seismic inputs, are derived by means of the following procedure:

- first, the convolution integral between the seismic fragility curves and seismic hazard curve allows to calculate the annual mean rate exceeding the limit state λ_{LS}, as expressed in Eq.(2):

$$\lambda_{LS}(EDP > y) = \int_0^\infty P(EDP > y \mid S_a(T) = x)\left|\lambda(\mathrm{d}S_a(T) > x)\right| \tag{2}$$

in which, $\lambda(\mathrm{d}S_a(T) > x)$ is the derivative of the hazard curve for $S_a(T)$ (i.e., the annual mean rate exceeding the specific value of the IM = $S_a(T) = x$ in Fig. 15) multiplied by an increment of $dS_a(T)$, and $P(EDP > y|S_a(T) = x)$ is the probability of the EDP exceeding y (i.e., a specific LS threshold) given a ground motion with $S_a(T) = x$. The term $P(EDP > y|S_a(T) = x)$ represents the fragility curves computed in Section 4 (Fig. 11-Fig. 14).

- then, by means of Poisson model, it is possible to compute the probabilities exceeding the LSs within the reference lifetime of 50 years, as expressed in Eq. (3):

$$P_f(50\text{years}) = 1 - \exp(-\lambda_{LS}(EDP > y)\cdot(50\text{years})) \tag{3}$$

Fig. 16 illustrates the seismic reliability results through seismic demand hazard curves of the structure under investigation for the different EDPs considered. In detail, Fig. 16 shows, for the three confinement models, the probabilities exceeding a given LS in 50 years related to the four IDIs, considering both the standard seismic design and proposed seismic design. As a result, the SP curves are different between the standard seismic design and proposed seismic design methodology since the plots present different orders of magnitude in terms of exceedance probabilities. It is also possible to observe that the LS1, LS2 and LS3 are always respected with higher safety margins for the proposed seismic design methodology.

Regarding the standard seismic design (Fig. 16- a),c),e),g)), the curves related to the three models have similar values of exceedance probabilities P_f(50 years) for all the LSs, i.e., in the range between 10^{-1}-10^{-2}. The SP curves respect the PO curve regarding the LS1, LS2 and LS3 and always fail with respect to the LS4. In fact, considering the FOLS and OLS performance levels (i.e., LS1 and LS2), the exceedance probabilities P_f(50 years) are, respectively, in the range P_f(50 years) = 0.06–0.1 (LS1) and P_f(50 years)= 0.02–0.04 (LS2) for the three models and the four IDIs. As for the LS3 (i.e., LSLS) at the 1st story, the SP curve is quite coincident with the PO curve regarding the model 1 (i.e., Saatcioglu & Razvi model), that leads always to the highest values. As for the NC performance level (i.e., LS4), the probability P_f(50 years) values are similar to the ones computed for the LS3 varying in a range between 0.01 and 0.02. Finally, the enveloped parameter IDI_{max} presents the highest values at each LS: mainly influenced by IDI_2 for the LS1 and LS2,

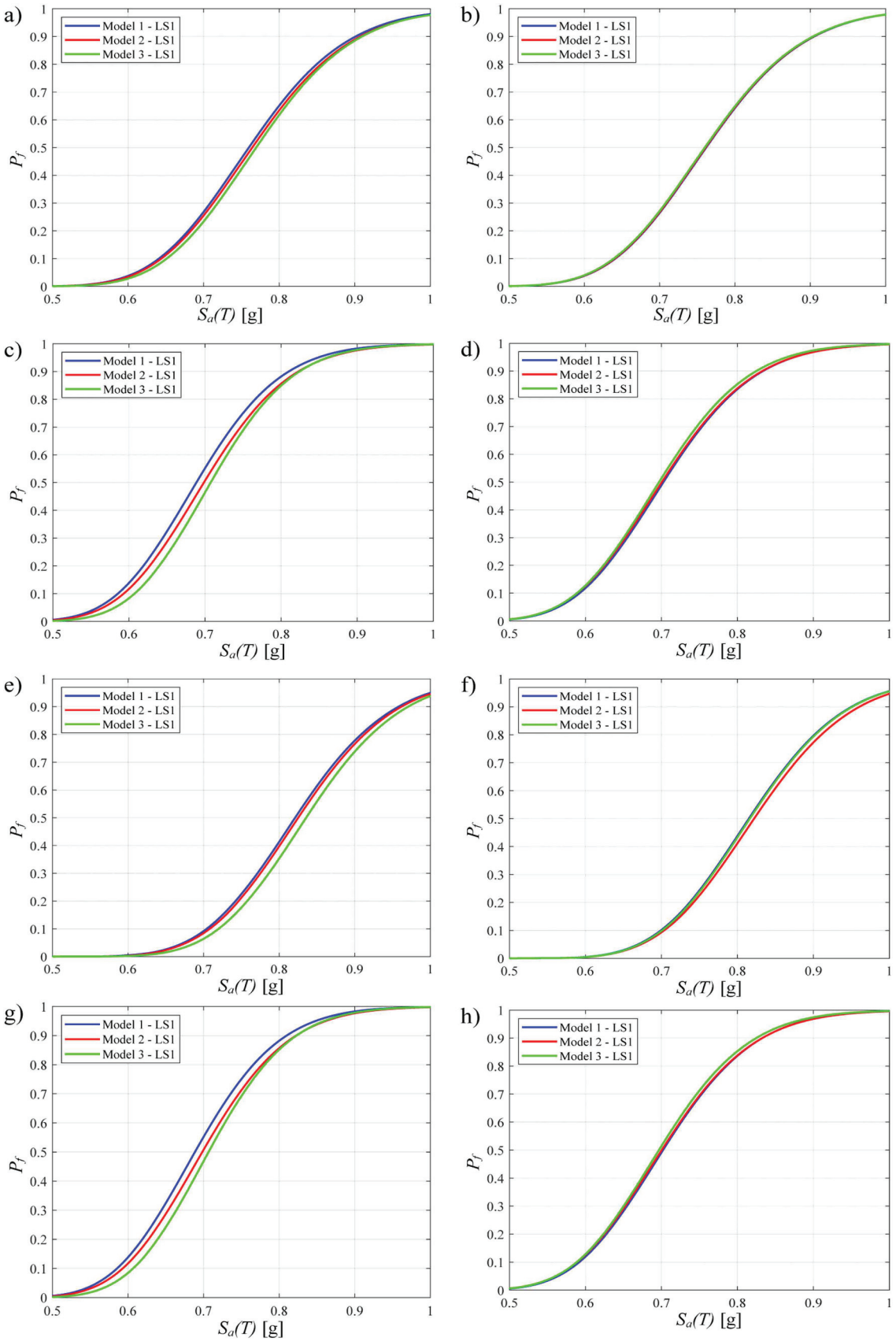

Fig. 11. Fragility curves of the a)-b) 1st story, c)-d) 2nd story, e)-f) 3rd story and g)-h) maximum for the LS1 threshold considering the three models (i.e., models 1, 2 and 3), the standard seismic design (left) and the proposed seismic design methodology (right).

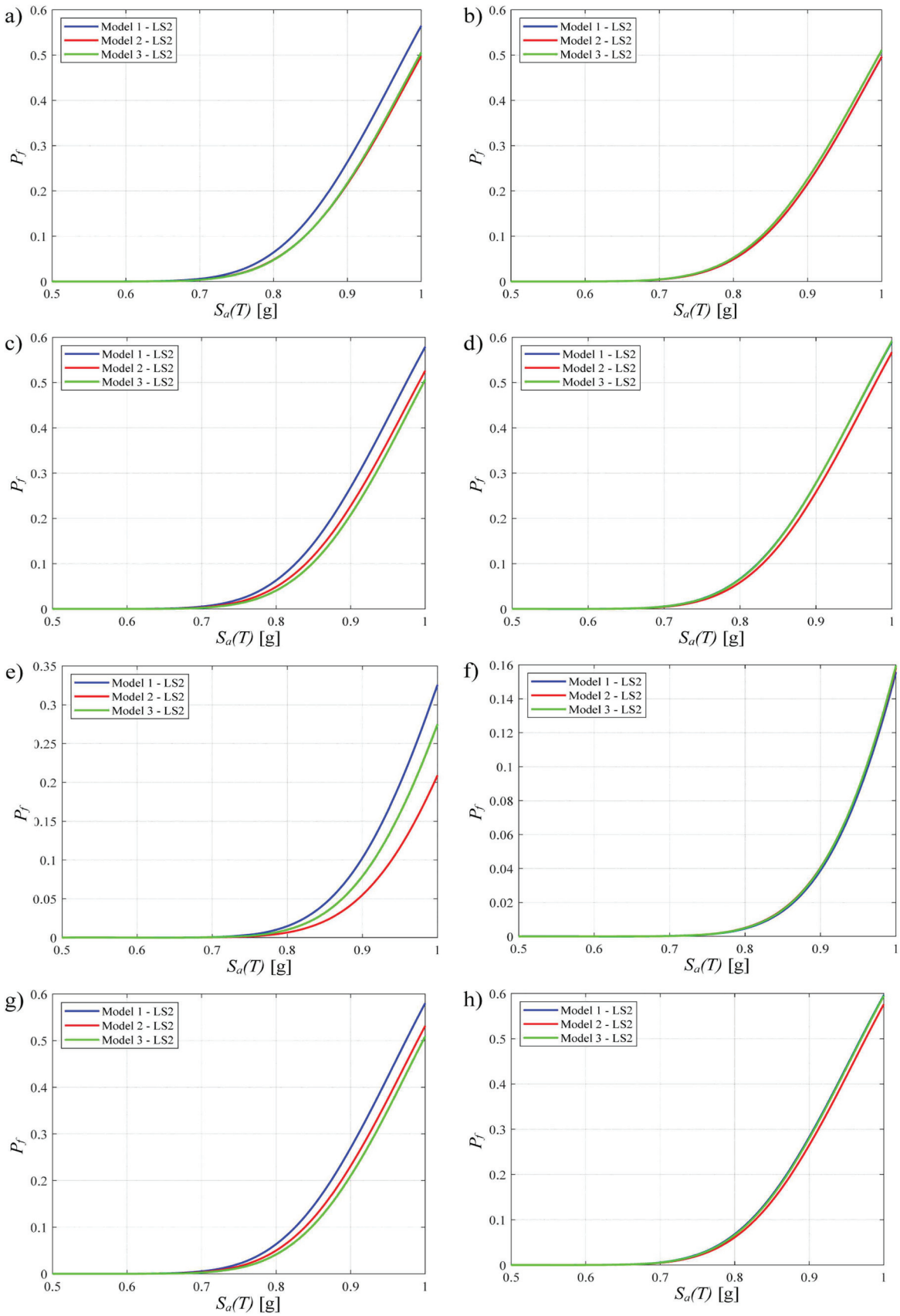

Fig. 12. Fragility curves of the a)-b) 1st story, c)-d) 2nd story, e)-f) 3rd story and g)-h) maximum for the LS2 threshold considering the three models (i.e., models 1, 2 and 3), the standard seismic design (left) and the proposed seismic design methodology (right).

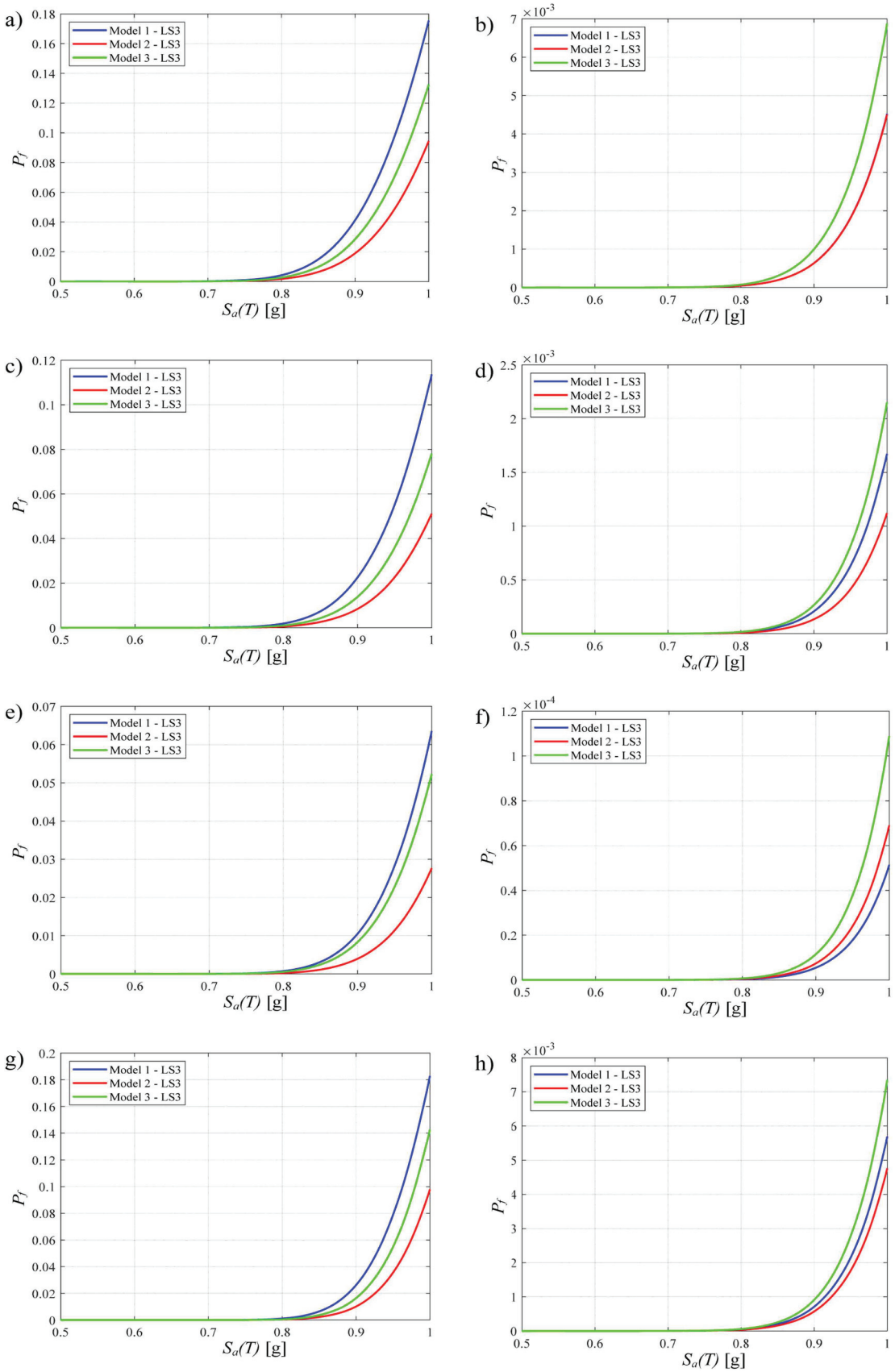

Fig. 13. Fragility curves of the a)-b) 1st story, c)-d) 2nd story, e)-f) 3rd story and g)-h) maximum for the LS3 threshold considering the three models (i.e., models 1, 2 and 3), the standard seismic design (left) and the proposed seismic design methodology (right).

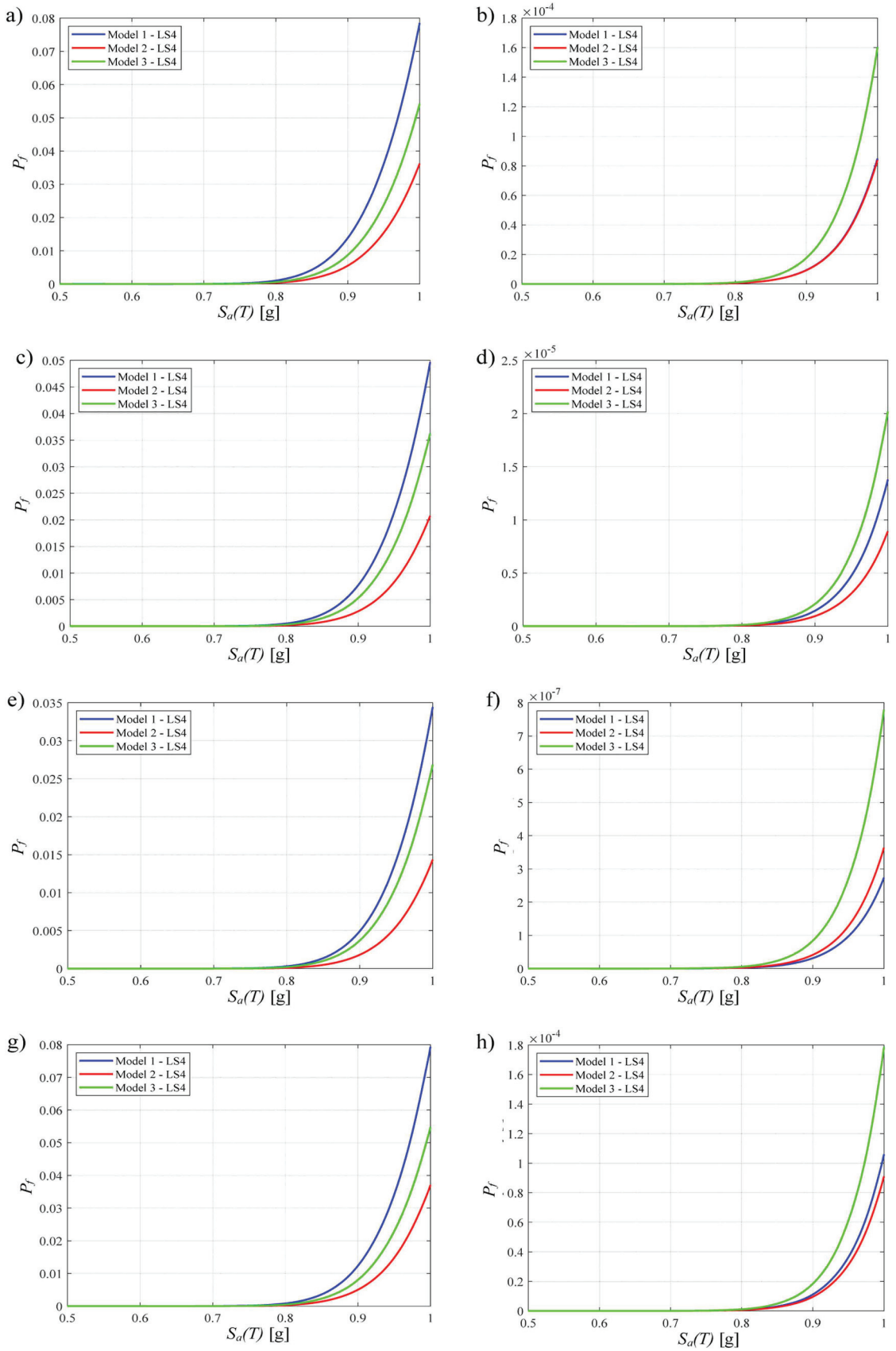

Fig. 14. Fragility curves of the a)-b) 1st story, c)-d) 2nd story, e)-f) 3rd story and g)-h) building for the LS4 threshold considering the three models (i.e., models 1, 2 and 3), the standard seismic design (left) and the proposed seismic design methodology (right).

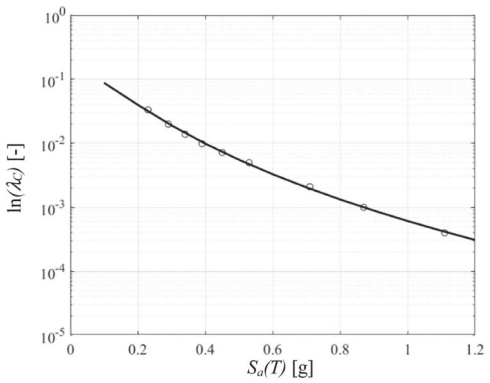

Fig. 15. L'Aquila seismic hazard curve.

whereas, more dependent on IDI_1 for the LS3 and LS4. All the results are in line with the seismic fragility curves previously computed.

Regarding the proposed seismic design (Fig. 16-b),d),f),h)), the SP curves computed at the LS1, LS2 and LS3 have probability P_f(50 years) values lower than the code objectives, respectively, variable in the ranges 0.06–0.1 (LS1), 0.02–0.04 (LS2) and 0.002–0.008 (LS3).

With reference to the NC performance level (i.e., LS4), the SP curves have much lower values of the exceedance probabilities P_f(50 years) in comparison to the previous LSs and always respect the PO curve. Specifically, the range of the probability is 0.0002–0.0004 for the EDP IDI_3, is around 10^{-3} for the EDP IDI_2, while, for the EDP IDI_1, the LS4 code threshold is respected also in case of the model 3 (i.e., NTC18/Parabola-rectangle model). Similarly, the enveloped parameter IDI_{max} presents the highest values at each LS: mainly influenced by IDI_2 for the LS1 and LS2, whereas, more dependent on IDI_1 for the LS3 and LS4. All the results confirm the seismic fragility results described in the previous section.

It is also noteworthy to underline that, although the model 3 (i.e., NCT2018/Parabola-rectangle model) always provides the highest values within the proposed seismic design, the differences (i.e., epistemic uncertainties) between the three confinement models are lower with respect to the standard seismic design, especially, for the LS1, LS2 and LS3. Therefore, the proposed seismic design leads to a reduction of the model uncertainties regarding the confinement models.

All the achieved results demonstrate that the overstrength effects due to the confined concrete behavior, especially, at member level (i.e., the overstrength in flexural resistance in the beams) are better accounted for in the proposed seismic design. This is testified by the fulfilment of the shear verifications considering the IDA outputs within the proposed seismic design to ensure more ductile mechanisms. In fact, the outcomes highlight the effectiveness of the proposed seismic design, for the frame under investigation, in improving the seismic performance, especially, in terms of ductility to respect the reliability objective levels. This proposed design approach covers the uncertainty on the possible effects deriving from the conccrete confinement (i.e., partially confined and confined concrete) in all structural elements and can be more relevant if the columns have higher axial force (i.e., larger υ_d), or the ultimate-to-yield strength ratio of the reinforcement steel is higher or for beams with lower base/height ratio. Moreover, if the aleatory uncertainties regarding the elastic and inelastic material properties had been considered, the SP curves deriving from the standard seismic design would have a lower safety margin with respect to the third LS (i.e., LSLS).

7. Conclusions

This study assesses the seismic reliability of a 2D RC MR frame located in a highly seismic zone in Italy. The main scope is to improve the design methodology considering explicitly the confinement effects within the seismic design. Specifically, the seismic reliability of a new regular RC MR frame, designed in a high ductility class, is compared with the one of the same frame designed considering the concrete confinement effects at structural and member level. In addition, three constitutive models are considered, denoted as model 1, model 2 and model 3. The proposed seismic design, combined with the three confinement models, and standard seismic design are implemented according to the codes. A set of 30 non-frequent natural ground motions is selected to develop the non-linear IDAs. The peak values in terms of the IDIs are adopted as EDPs.

From the IDA curves, the following results can be summarised:

- a relevant reduction of collapse cases with respect to shear verifications is observed when confinement effects are explicitly included in the seismic design due to the higher resistances and ductility capacities characterising the structural elements, especially, for the beams;
- the EDP IDI_2 at the second floor shows the highest values, whereas the IDA curves related to the EDP IDI_1 are characterized by the highest dispersions;
- the results of the three confinement models show some differences in both the numerical response and collapse cases.

Subsequently, appropriate LS thresholds have been assumed to define the seismic fragility curves taking into account the collapse cases. The fragility curves show:

- important differences between the two design methodologies and the three confinement models, especially, for high LS thresholds with a non-linear structural response (i.e., LS3 and LS4);
- the probabilities strongly decrease for the proposed seismic design as the LS threshold increases. The highest values are generally reached by the EDP IDI_2 for the LS1 and LS2, whereas, by the EDP IDI_1 for the LS3 and LS4. In addition, the model 1 leads to the highest values for the standard seismic design, whereas the model 3 provides the highest values for the proposed seismic design.

Successively, the seismic reliability curves have been derived and the following conclusions can be drawn:

- the seismic performance, computed in 50 years within the standard seismic design, is able to respect the LS1, LS2 and LS3 but always fails with respect to the LS4;
- the seismic reliability strongly improves in terms of ductility respecting all the LSs within the proposed seismic design. In detail,

Table 5
Probabilities exceeding LS thresholds within 50 years provided by [30–32,72,55,65,74].

Performance Level	Limit State	P_f (50 years) [-]
Fully Operational	LS1	5.00E-01
Operational	LS2	1.60E-01
Life Safety	LS3	2.20E-02
Near Collapse	LS4	1.50E-03

Table 4
Values of λ_c and pseudo-accelerations $S_a(T)$.

λ_c [-]	0.0004	0.0010	0.0021	0.0050	0.0072	0.0099	0.0139	0.0200	0.0335
$S_a(T)$ [g]	1.11	0.87	0.71	0.53	0.45	0.39	0.34	0.29	0.23

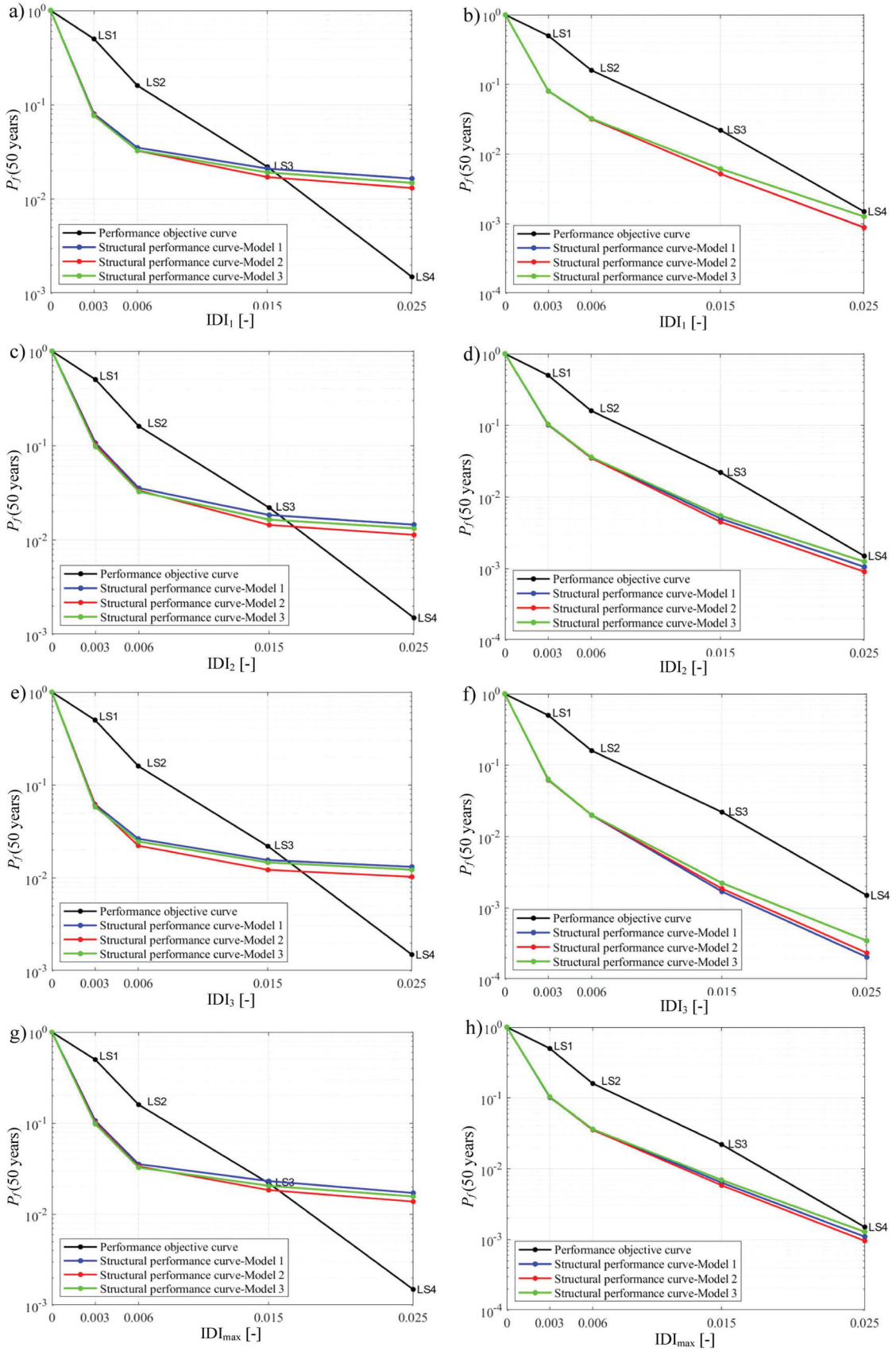

Fig. 16. Probabilities exceeding the four Limit States for the three confinement models in 50 years in terms of the IDIs referred to the a)-b)1st story, c)-d) 2nd story, e)-f) 3rd story and g)-h) maximum - the standard seismic design (left) vs the proposed seismic design methodology (right).

there is a reduction of almost one order of magnitude at the LS4 if the confinement effects are explicitly included in the seismic design;
- the differences between the three constitutive models for the confined concrete (i.e., epistemic uncertainties) decrease if the confinement effects are included in the seismic design.

All the achieved results demonstrate that, for the frame under investigation, the proposed seismic design can improve the seismic performance, especially, in terms of ductility to respect the reliability objective levels since the overstrength effects of the confined concrete behavior are better accounted for, especially, at member level (i.e., the overstrength in flexural resistance in the beams). This is testified by the fulfilment of the shear verifications to ensure more ductile mechanisms. The proposed design approach covers the uncertainty on the possible effects deriving from the conccrete confinement (i.e., partially confined and confined concrete) in all structural elements and can be more relevant for higher values of the axial force in columns (i.e., larger υ_d), or of the ultimate-to-yield strength ratio in the reinforcement steel or for beams with lower base/height ratio. Moreover, if the aleatory uncertainties regarding the elastic and inelastic material properties had been considered, the seismic performance of the structure under investigation, designed within the standard seismic design, would have a lower safety margin with respect to the third LS (i.e., LSLS).

CRediT authorship contribution statement

Miceli Elena: Supervision, Visualization, Conceptualization, Methodology, Software, Writing- Original draft, Data curation, Writing-Reviewing and Editing, Validation, Investigation, Formal analysis. **Ferrara Salvatore:** Methodology, Investigation, Formal analysis. **Castaldo Paolo:** Supervision, Conceptualization, Methodology, Reviewing and Editing, Validation.

Declaration of Competing Interest

No conflict of interest.

Data Availability

Data will be made available on request.

Acknowlegements

This study was carried out within the RETURN Extended Partnership and received funding from the European Union Next-GenerationEU (National Recovery and Resilience Plan – NRRP, Mission 4, Component 2, Investment 1.3 – D.D. 1243 2/8/2022, PE0000005).

References

[1] Ni P, Li J, Hao H, Yan W, Du X, Zhou H. Reliability analysis and design optimization of nonlinear structures. Reliab Eng Syst Saf 2020;198:106860.
[2] Polese M, Verderame GM, Mariniello C, Iervolino I, Manfredi G. Vulnerability curves for gravity load designed RC buildings in Naples – Italy. J Earthq Eng 2008; 12(S2):234–45.
[3] Hognestad E. A study of combined bending and axial load in reinforced concrete members. Bulletin Series No, 399. Urbana: Univ. of Illinois Engrg. Experimental Station; 1951. p. 111.
[4] Chan WWL. The ultimate strength and deformation of plastic hinges in reinforced concrete frameworks. Mag Concr Res 1955;Vol. 7(No. 21):121–32. Nov. 1955.
[5] Roy HEH, Sozen MA. Ductility of concrete. Am Concr Inst, Acids Spec Publ 1965; vol. SP-012:213–35.
[6] Kent DC, Park R. Flexural members with confined concrete. J Struct Div, ASCE 1971;Vol. 97:1969–90. ST7, July 1971.
[7] Sargin M, Ghosh SK, Handa UK. Effects of lateral reinforcement upon the strength and deformation properties of concrete. Mag Concr Res 1971;Vol. 28(No.75-76): 99–110. June-Sept. 1971.
[8] Vallenas J.M., Bertero V.V., Popov E.P. (1977), Concrete Confined by Rectangular Hoops and Subjected to Axial Load", Earthquake Engineering Research Center, College of Engineering, University of California, Berkeley, U.S.A., Report No. UCB/EERC-77/13, August 1977, 114.
[9] Sheikh SA, Uzumeri SM. Strength and ductility of tied concrete columns. ASCE J Struct Div 1980;vol. 106(5):1079–102.
[10] Scott BD, Park R, Priestley MJN. Stress-strain behavior of concrete confined by overlapping hoops at low and high strain rates. Acids J 1982;79(1):13–27.
[11] Mander JB, Priestley MJ, Park R. Fellow, theoretical stress-strain model for confined concrete. J Struct Eng, ASCE 1988;114(8):1804–26.
[12] Yong YK, Nour MG, Nawy EG. Behavior of laterally confined high-strength concrete under axial loads. J Struct Div, ASCE 1988;V. 114:332–51. No. ST2, Feb. 1988.
[13] Saatcioglu M, Razvi S. Strength and ductility of confined concrete. J Struct Eng 1992:1590–607.
[14] Attard MM, Setunge S. Stress-strain relationship of confined and unconfined concrete. Acids Mater J 1996;93(5):432–42.
[15] Montoya Esneyder, Vecchio Frank J, Sheikh Shamim A. Compression field modeling of confined concrete: constitutive models. J Mater Civ Eng 2006;18(4): 510–7.
[16] Riederer KA. Assessment of confinement models for reinforced concrete columns subjected to Seismic loading (December) Master Appl Sci Univ Br Columbia 2006 (December).
[17] Li W, Sun L, Zhao J, Lu P, Yang F. Seismic performance of reinforced concrete columns confined with two layers of stirrups, Research article. Struct Des Tall Spec Build 2018.
[18] Ahmad N, Rizwan M, Ilyas B, Hussain S, Khan MU, Shakeel H, et al. Nonlinear modeling of RC substandard beam-column joints for building response analysis in support of seismic risk assessment and loss estimation. 4 October Res Artic 2022. 4 October.
[19] Castaldo P, Gino D, Bertagnoli G, Mancini G. Resistance model uncertainty in nonlinear finite element analyses of cyclically loaded reinforced concrete systems. Eng Struct 2020;211:110496.
[20] Bojórquez J, Ponce S, Ruiz SE, Bojórquez E, Reyes-Salazar A, Barraza M, et al. Structural reliability of reinforced concrete buildings under earthquakes and corrosion effects. Eng Struct 2021;237:112161.
[21] Castaldo P, Palazzo B, Ferrentino T. Seismic reliability-based ductility demand evaluation for inelastic base-isolated structures with friction pendulum devices. Earthq Eng Struct Dyn 2017;46:1245–66.
[22] Kalantari A, Roohbakhsh H. Expected seismic fragility of code-conforming RC moment resisting frames under twin seismic events. J Build Eng 2020;28:101098.
[23] Yön B, Calayır Y. Effects of confinement reinforcement and concrete strength on nonlinear behaviour of RC buildings. Comput Concr 2014;Vol. 14(No. 3):279–97.
[24] Aydemir C, Zorbozan M. Uncertainty analysis of flexural overstrength ratio for RC columns. J Struct Eng 2012;138(8):1042–53.
[25] Hassan WM, P.E PhD, M.ASCE SE, Elmorsy M. Probabilistic beam–column joint model for seismic analysis of concrete frames. 04022011-1 J Struct Eng, ASCE 2022;148(4). 04022011-1.
[26] C.L. Segura Jr., S. Sattar, Uncertainty in the Seismic response of Reinforced Concrete structures due to material variability, 17th World Conference on Earthquake Engineering, 17WCEE - Sendai, Japan, Paper N° C000807, Registration Code: S-A01917, September 13th to 18th 2020.
[27] Buratti N, Ferracuti B, Savoia M. Response Surface with random factors for seismic fragility of reinforced concrete frames, N. Buratti et al. Struct Saf 2010;32:42–51.
[28] Radujković A, Starčev-Ćurčin A, Laðinović Đ, Džolev I. Assessment of RC frame seismic performance related to confined concrete models. Conference Paper; 2017.
[29] Eurocode 2, Design of concrete structures - Part 1–1: General rules and rules for buildings, UNI-EN1992–1-1, EC2–1-1, Update January 1993.
[30] Eurocode 8, Design of structures for earthquake resistance - Part 1: General rules - seismic actions and rules for buildings, UNI EN 1998–1, EC8–1, Update March 2007.
[31] Ministry of Infrastructure and Transport (2018). Italian Technical Standards for Construction - NTC18, Rome, Italy.
[32] Application Circular of the NTC2018, Update February 2019.
[33] Paulay T, Priestley MJN. Seismic design of reinforced concrete and masonry buildings. New York: Wiley; 1992.
[34] Galasso C, et al. Uncertainly analysis of flexural overstrength for capacity design of RC beams. J Struct Eng 2014;140(7).
[35] I.K. Sudarsana, I.A.M. Budiwati, P.W. Aditya, Effect of column to beam strength ratio on performance of reinforced concrete frames, in: Proceedings Of the 1st International Conference On Engineering Technology And Industrial Application, Surakarta, Indonesia, 2014.
[36] Ghorbanzadeh M, Khoshnoudian F. The effect of strong column-weak beam ratio on the collapse behaviour of reinforced concrete moment frames subjected to near-field earthquakes (AHEAD-OF-PRINT) J Earthq Eng 2020:1–24.
[37] Kim C-S, et al. Column-to-beam flexural strength ratio for performance-based design of RC moment frames. J Build Eng 2022;46103645.
[38] Park, R., (1996). Explicit incorporation of element and structure overstrength in the design process. Proceedings of the 11th WCEE. IAEE, Acapulco, Mexico, Paper.
[39] D. Vamvatsikos and C.A. Cornell, Incremental Dynamic Analysis, Department of Civil and Environmental Engineering, Stanford University, CA 94305–4020, U.S.A, 2002.
[40] SAP2000 v20, Integrated Solution for Structural Analysis and Design, Documentation, 2018.
[41] Panagiotakos TB, Fardis MN. Deformations of reinforced concrete members at yielding and ultimate. Acids Struct J 2001;98(2):135–48.
[42] Takeda T, Sozen MA, Nielsen NN. Reinforced concrete response to simulated earthquakes. J Struct Div 1970;96:2557–73.

[43] M. Fardis, Seismic design, assessment and retrofitting of concrete buildings, Springer, 2009.
[44] K.A. Porter, An Overview of PEER's Performance-Based Earthquake Engineering Methodology, Ninth International Conference on Applications of Statistics and Probability in Civil Engineering, ICASP9, San Francisco, July 6–9 2003.
[45] Porter K, Kennedy R, Bachman R. Creating fragility functions for performance-based earthquake engineering. Earthq Spectra 2007;Volume 23(No. 2):471–89.
[46] Nilesh GC, Abhijeet GA, Sumant KK. Scaling Of ground motions for performing incremental dynamic analysis of RC framed structures. Int J Adv Res Ideas Innov Technol 2017.
[47] Aslani H, Miranda E. Probability-based seismic response analysis. Eng Struct 2005;27(8):1151–63.
[48] Shome N, Cornell CA, Bazzurro P, Carballo JE. Earthquake, records and nonlinear responses. Earthq Spectra 1998;14(3):469–500.
[49] Luco N, Cornell CA. Structure-specific scalar intensity measures for near-sorce and ordinary earthquake ground motions. Earthq Spectra 2007;23(2):357–92.
[50] Auad G, Castaldo P, Almazán JL. Seismic reliability of structures equipped with LIR-DCFP bearings in terms of superstructure ductility and isolator displacement. Earthq Eng Struct Dyn 2022;51(13):3171–214.
[51] fib Model Code for Concrete Structures 2010 . fib 2013. Lausanne.
[52] Gino G, Miceli E, Castaldo P, Recupero A, Mancini G. Strain-based method for assessment of global resistance safety factors for NLNAs of reinforced concrete structures. Eng Struct 2024;304:117625. https://doi.org/10.1016/j.engstruct.2024.117625.
[53] JCSS. JCSS Probabilistic Model Code. 2001.
[54] Eurocode 8, Design of structures for earthquake resistance - Part 3: Assessment and retrofitting of buildings, UNI EN 1998–3, EC8–3, 2005.
[55] FEMA 274, NEHRP Commentary on the Guidelines for the Seismic Rehabilitation of Buildings, October 1997.
[56] Biskinis DE, Roupakias GK, Fardis MN. Degradation of shear strength of reinforced concrete members with inelastic cyclic displacements. Acids Struct J 2004.
[57] Bazzurro P, Cornell CA, Shome N, Carballo JE. Three proposals for characterizing MDOF nonlinear seismic response. J Struct Eng 1998;124(11):1281–9.
[58] Castaldo P, Palazzo B, Alfano G, Palumbo MF. Seismic reliability-based ductility demand for hardening and softening structures isolated by friction pendulum bearings. Struct Control Heal Monit 2018;25:2256.
[59] Castaldo P, Tubaldi E. Influence of FPS bearing properties on the seismic performance of base-isolated structures. Earthq Eng Struct Dyn 2015;44:2817–36.
[60] Tubaldi E, Ragni L, Dall'Asta A. Probabilistic seismic response assessment of linear systems equipped with nonlinear viscous dampers. Earthq Eng Struct Dyn 2015;44(1):101–20.
[61] Castaldo P, Amendola G, Palazzo B. Seismic fragility and reliability of structures isolated by friction pendulum devices: seismic reliability-based design (SRBD). Earthq Eng Struct Dyn 2017;46:425–46.
[62] Karavasilis T, Seo C. Seismic structural and non-structural performance evaluation of highly damped self-centering and conventional systems. Eng Struct 2011;33(8):2248–58.
[63] Castaldo P, Alfano G. Seismic reliability-based design of hardening and softening structures isolated by double concave sliding devices. Soil Dyn Earthq Eng 2020;129:105930.
[64] MATLAB R2018b software, The MathWorks In., 1994–2018.
[65] SEAOC Vision. Committee, Performance-based seismic engineering, Report prepared by Structural Engineers Association of California. Sacram, CA 2000:1995.
[66] Collins KR, Wen YK, Foutch AD. Dual-level seismic design: a reliability-based methodology. Earthq Eng Struct Dyn 1997.
[67] C.A. Cornell and F. Jalayer, A Technical Framework for Probability-Based Demand and Capacity Factor Design (DCFD) Seismic Formats, Pacific Earthquake Engineering Research Center, Department of Civil and Environmental Engineering Stanford University, 2003.
[68] Aoki Y, Ohashi Y, Fujitani H, Saito T, Kanda J, Emoto T, et al. Target Seism Perform Lev Struct Des Build 2000.
[69] Cornell CA, Krawinkler H. Progress and challenges in seismic performance assessment. PEER Cent N 2000;4(1):1–3.
[70] Bertero RD, Bertero VV. Performance-based seismic engineering: the need for a reliable conceptual comprehensive approach. Earthq Eng Struct Dyn 2002;31:627–52.
[71] K. Collins, B. Stojadinovic, Limit states for performance-based design, Proceedings of 12 WCEE, Auckland, New Zealand, 2000.
[72] ASCE STANDARD, Minimum Design Loads for Buildings and Other Structures, American Society of Civil Engineers, SEI 7–10, 2010.
[73] National Institute of Geophysics and Volcanology (INGV), Department of Civil Protection, Annex A and B to the Technical Standards for Construction: Seismic hazard, NTC08, Decree of the Ministry of Infrastructures, GU n.29, 04/02/2008.
[74] Eurocode 0, Basis of Structural Design, CEN, European Committee for Standardization, Final draft, Brussels, 2006.